

THE GREAT COMET OF 1106, A CHINESE COMET OF 1138, AND DAYLIGHT COMETS IN LATE 363 AS KEY OBJECTS IN COMPUTER SIMULATED HISTORY OF KREUTZ SUNGRAZER SYSTEM

ZDENEK SEKANINA¹ AND RAINER KRACHT²

¹Jet Propulsion Laboratory, California Institute of Technology, 4800 Oak Grove Drive, Pasadena, CA 91109, U.S.A.

²Ostlandring 53, D-25335 Elmshorn, Schleswig-Holstein, Germany

Version July 4, 2022

ABSTRACT

We present the results of our orbital computations in support of the recently proposed contact-binary model for the Kreutz sungrazer system (Sekanina 2021, 2022). We demonstrate that comet Ikeya-Seki (C/1965 S1) previously passed perihelion decades after the Great Comet of 1106 (X/1106 C1) and argue that, like the Great September Comet of 1882 (C/1882 R1), it evidently was a fragment of the comet recorded by the Chinese in September 1138. The 1106 sungrazer appears instead to have been the previous appearance of the Great March Comet of 1843 (C/1843 D1). With no momentum exchange involved, fragments of a Kreutz sungrazer breaking up tidally near perihelion are shown to end up in orbits with markedly different periods because their centers of mass are radially shifted by a few kilometers relative to the parent. The daylight comets of AD 363, recorded by a Roman historian, are accommodated in our computations as the first appearance of the Kreutz sungrazers after their bilobed progenitor’s breakup. We link the 1843–1106–363 (Lobe I) and 1882–1138–363 (Lobe II) returns to perihelion by single nongravitational orbits and gravitationally with minor center-of-mass shifts acquired in fragmentation events. We also successfully model the motion of Aristotle’s comet as the rotating progenitor that at aphelion split (at a few m s^{-1}) into the two lobes, the precursors of, respectively, the 1843 and 1882 sungrazers; and provide a 1963–1041–363 link for comet Pereyra (C/1963 R1). Material fatigue could contribute to sungrazers’ fragmentation throughout the orbit, including aphelion. — Continuing problems with the nongravitational law in orbit software are noted.

Subject headings: comets general: Kreutz sungrazers; comets individual: 372 BC, 363, 1041, X/1106 C1, 1138, C/1843 D1, C/1882 R1, C/1963 R1, C/1965 S1; methods: data analysis

1. INTRODUCTION

Among the Kreutz sungrazers seen in the past 200 years, two objects have stood out as by far the intrinsically brightest and presumably the most massive: the Great March Comet of 1843 (C/1843 D1) and the Great September Comet of 1882 (C/1882 R1). Moving about the Sun in somewhat different orbits (though sharing a common line of apsides), they are the quintessential members of two fundamental subgroups or populations, I and II, respectively. Their possible history was described more than 50 years ago by Marsden (1967). Although the number of known populations has gradually been growing (e.g., Marsden 1989), Populations I and II have remained. Bright Kreutz sungrazers have repeatedly been observed to fragment or disintegrate at perihelion, but the existence of the distinct populations cannot be explained by perihelion breakups, unless unrealistically long periods of time are invoked.

While the populations are in principle understood as products of cascading fragmentation at all heliocentric distances, with the primary breakup in the general proximity of *aphelion* (Sekanina 2002; Sekanina & Chodas 2004, 2007), a meaningful modeling of the Kreutz system’s evolution requires at least limited knowledge of the history of its members. Given that the typical orbital periods of the Kreutz comets exceed 700 yr, the parent objects of the 19th to 21st century sungrazers are necessarily historical comets, for which little, if any, information is available.

2. PAST WORK RELATED TO THE COMET OF 1106

The Great Comet of 1106 (X/1106 C1), long suspected from historical records to have been a sungrazer (e.g., Pingré 1783, Hall 1883, Kreutz 1888, 1901), should constitute an integral part of any evolutionary investigation of the Kreutz system. Although limited data are available on the comet’s tail, no orbit could be computed. Granted it indeed was a Kreutz comet, the issue of whether it was a previous appearance of the Great March Comet of 1843 (of Population I) or the Great September Comet of 1882 (of Population II) has long been a point of contention.

A pivotal role in efforts to settle this issue has in fact been played by another sungrazer, comet Ikeya-Seki (C/1965 S1), whose orbit in many respects resembles that of the 1882 comet so closely that it has served as an indispensable proxy because of its much higher accuracy. Perihelion fragmentation and the resulting post-perihelion nucleus multiplicity complicate matters in either case, but comet Ikeya-Seki was observed after perihelion to possess two persisting fragments, while the 1882 sungrazer displayed up to six. Integrating the orbit of the primary nucleus of Ikeya-Seki back in time, Marsden (1967) established that it would have previously been at perihelion in March 1115 or September 1116 depending on whether the relativistic effect was or was not included. His integration of Kreutz’s (1891) nonrelativistic orbit for the primary nucleus (No. 2 in Kreutz’s notation) of the 1882 comet gave the previous perihelion in April 1138. Marsden concluded that the Great Comet of 1106 “seems by far the most promising candidate for the previous ap-

pearance of comet [Ikeya-Seki]” and that it was “virtually proven that [the 1882 comet and Ikeya-Seki] were indeed one at their previous approach to the Sun.”

While evidence for the second conclusion is strong, the first is questionable because of as yet unresolved issues in the orbital motions of the 1882 comet and Ikeya-Seki. While for the first comet we have nothing to add to Kreutz’s (1891) results, we develop a novel technique to apply to the orbit of comet Ikeya-Seki in order to settle the question of whether or not the 1106 comet was this sungrazer’s previous appearance.

The “best-determined” orbit of each nucleus fragment of the Great September Comet of 1882 or comet Ikeya-Seki was computed (by Kreutz or by Marsden) by linking the comet’s pre-fragmentation astrometric positions before perihelion with that fragment’s positions after perihelion. On the one hand, such an orbital solution is — to say the least — problematic because it smoothes the motion prior to and after the point of dynamical discontinuity associated with the splitting — the very effect of interest. On the other hand, the options of overcoming the discontinuity problem are in practice very limited because separate preperihelion and post-perihelion orbital arcs are inadequate to serve as a basis for accurate orbital-period determination.

Although subject to occasional criticism, Marsden’s (1967, 1989) preference for the 1106 comet as the parent to the 1882 sungrazer and Ikeya-Seki’s comet (rather than to the 1843 comet) was incorporated into the two-superfragment model of the Kreutz system, proposed by Sekanina (2002) and implemented by Sekanina & Chodas (2004). The subsequently developed alternative model (Sekanina & Chodas 2007) adopted the 1106 comet as the parent to the 1843 comet. Following the appearance of comet Lovejoy (C/2011 W3) and other relevant new developments in the past 10 years, these models were upgraded by the recent introduction of a novel conceptual model (Sekanina 2021; referred to hereafter as Paper 1), in which the birth of the Kreutz system was linked to a breakup of the *contact-binary* progenitor near aphelion about two millennia ago. The 1106 comet was presented in this model as the most massive fragment of Lobe I and the precursor of the 1843 comet. The perihelion time of the 1106 comet was then found to have fitted a uniform time sequence of three generations of Population I fragments, derived from Aristotle’s comet of 372 BC as the progenitor. However, temporal effects triggered by the indirect planetary perturbations, by the outgassing-driven nongravitational forces, and/or by other possible mechanisms in the course of recurrent near-perihelion fragmentation events were all ignored, and this is being corrected in the present paper.

3. NEW EVIDENCE FROM THE ORBITAL MOTION OF COMET IKEYA-SEKI

The 119 observations used by Marsden (1967) to compute the orbit of the primary nucleus, A, of Ikeya-Seki are all included in the list presented in the Minor Planet Center’s database¹. The list contains a total of 129 astrometric observations, of which 78 are preperihelion data points from a period of 1965 September 21 through October 16; nine data points from the early post-perihelion

period of October 28 through November 1, before discovery of the companion nucleus, B; and 42 positions of nucleus A from November 5 on. The actual number of reported astrometric observations was much higher, but none of the grossly inaccurate ones made it into the list. For example, missing are 23 of 27 positions originally published by the Central Bureau for Astronomical Telegrams on 1965 December 1 and all of those reported on December 17 and 30 (Gingerich 1965, Marsden 1965).

The key astrometric observations were made by Z. M. Pereyra and J. J. Rodríguez with the 33-cm f/10.5 astrograph of the Córdoba Observatory (Pereyra 1971): the first measured images were exposed by Pereyra on 1965 September 21.38 UT, less than three days after discovery; the last preperihelion and the first post-perihelion observations were made by Rodríguez on October 16.36 and 28.35 UT, respectively. The length of the preperihelion arc covered by the observations was merely 25 days. Further positional data in the early post-perihelion period, until November 1 (11 days after perihelion), were secured by Roemer (Roemer & Lloyd 1966) and by Lourens (1966). The secondary nucleus B was detected first on November 4.53 UT (Pohn 1965), but no astrometry was available from the period before November 12. The last reduced images of either fragment were acquired by Tammann (1966) with the Palomar Observatory’s 122-cm Schmidt telescope on 1966 January 14.33 UT, 85 days after perihelion;² they were measured by Marsden (1967). Overall, the comet’s orbital arc covered by the astrometric observations extends over 115 days; however, there is a data gap from 5 days before to 7 days after perihelion.

3.1. Approximating the Motion of the Pre-Split Nucleus

Our first objective was an in-depth review of the orbit of comet Ikeya-Seki based on the available set of preperihelion observations to confirm that they were utterly inadequate for determining the comet’s past motion. We tested the veracity of this conclusion by deriving several orbital solutions. Our computer code accounted for the perturbations by the planets, Pluto, and the three most massive asteroids, and for the relativistic effect. A general solution using all 78 preperihelion data points left residuals from three observations that exceeded 4” in one coordinate, and these were subsequently removed from the set. Eventually we obtained the orbital period from solutions based on 78, 75, 74, 72, and 70 data points. Summarized in Table 1, they show that the orbital period came out to be indeterminate, with enormous mean errors, confirming that this was not the way to proceed.

Instead, we followed a rather different path. We began by assuming, for the sake of argument, that the 1106 comet *was* the previous appearance of Ikeya-Seki, as suggested by Marsden (1967). We subtracted the Julian date of the perihelion time of the 1106 comet, nominally 1106 January 26 according to Hasegawa & Nakano (2001), from the Julian date of the 1965 perihelion passage of comet Ikeya-Seki to yield a pre-split barycentric orbital period of $P_{\text{bar}} = 859.68$ years, equivalent to a barycentric reciprocal semimajor axis of

² Porter (1967) noted that the comet was seen on films exposed with the Baker-Nunn cameras at two stations of the Smithsonian Astrophysical Observatory in late January and, possibly, mid-February, but none of these images was ever measured.

¹ See https://minorplanetcenter.net/db_search.

Table 1
Osculating Orbital Period of Comet Ikeya-Seki
from Preperihelion Observations
(Epoch 1965 Oct 7.0 TT)

Number of astrometric positions used	Orbital period, P_{osc} (yr)	Mean residual
78	980 ± 176	$\pm 1''.52$
75	1181 ± 408	$\pm 1''.41$
74	1426 ± 343	$\pm 1''.39$
72	1568 ± 468	$\pm 1''.33$
70	1442 ± 732	$\pm 1''.27$

$(1/a)_{\text{bar}} = +0.011055 \text{ AU}^{-1}$. With Everhart & Raghavan’s (1971) barycentric correction for the epoch of 1965 Oct 7.0 TT equaling $u_b = -0.000255 \text{ AU}^{-1}$, this exercise led to an osculating reciprocal semimajor axis of $(1/a)_{\text{osc}} = +0.010800 \text{ AU}^{-1}$ and an orbital period of $P_{\text{osc}} = 891$ years.

We next employed this value of $(1/a)_{\text{osc}}$ in *forced* orbital solutions to examine the degree of compatibility of the comet’s preperihelion astrometric observations with the premise on its previous perihelion passage in 1106. We found that *all 78 fitted this premise* to within $\pm 4''$ and 74 to within $\pm 3''.5$, a greater degree of conformity than in the formally optimized solutions in Table 1. This implied that the orbital periods much longer than 900 years were unrealistic.

We accepted that the comet’s fragmentation had taken place at a time of less than one hour from perihelion (Sekanina 1982, Sekanina & Chodas 2007) and pursued an objective of deriving an orbital period that was representative of the comet’s true motion before splitting, thus eliminating or mitigating the problems that plagued the computations leading to the unsatisfactory results in Table 1. We based our strategy on the fact that orbital positions of the most massive fragment of a split comet get affected by the fragmentation event only gradually, a number of days, if not weeks, later. This is documented by an often considerable lapse of time between the breakup (as determined by an appropriate method) and the first detection of nucleus duplicity (or multiplicity).³ For example, a typical nuclear fragment’s velocity of 1 m s^{-1} relative to the comet’s center of mass would not generate a potentially measurable position shift exceeding, say, 1000 km (equivalent in an extreme case to a projected position shift of $\sim 3''$ at a geocentric distance of 0.5 AU) until approximately 12 days after the breakup, which for Ikeya-Seki would be November 2.

This kind of argument led us to a conclusion that the comet’s credible pre-split orbital period could successfully be approximated by extrapolating a sequence of orbital runs, each of which links the set of preperihelion astrometric observations with a different set of *early* post-perihelion observations. We obtained four such sets of orbital solutions based on the 72 preperihelion data linked with, successively, two post-perihelion observations made on October 28 (the earliest post-perihelion data); four observations from October 28–29; six observations from

October 28–31; and nine observations from October 28–November 1. If these early post-perihelion observations are accurate, the runs should offer a set of barycentric orbital periods, P_{bar} , and times of the previous perihelion, T_{prev} , that display a systematic trend when plotted as a function of the termination date. Extrapolation of these values of P_{bar} and T_{prev} back to the termination date equaling the time of fragmentation should provide the desired credible estimates of the pre-split values. The values of P_{bar} and T_{prev} derived from runs whose termination dates are located beyond this early post-perihelion period are expected to be noisy, slowly converging to Marsden’s (1967) values for nuclear fragment A, and of lesser interest to this numerical exercise.

The results are presented in Table 2. The individual columns list: the time of termination observation, t_{fin} , and its reference to the perihelion time, $t_{\text{fin}} - T$ (the first observation, t_{first} , having always been September 21.38 UT and $t_{\text{first}} - T = -29.80$ days); the osculation value of the reciprocal semimajor axis, $(1/a)_{\text{osc}}$, for the epoch of 1965 October 7.0 TT and its mean error; the corresponding past barycentric value, $(1/a)_{\text{bar}}$; the past barycentric orbital period, P_{bar} , and its mean error; the derived nominal time of the previous perihelion passage, T_{prev} ; the mean residual of the orbital solution; the number of observations used, separately before and after perihelion; and the computed offset of the secondary nucleus B from the primary A at t_{fin} . It is a measure of the offset of A from the center of mass of the pre-split comet, which is expected to be its very small, approximately proportionate fraction.

For the sake of comparison, the first row of the table shows yet another useless solution based solely on the preperihelion observations. The numbers in the subsequent rows show that adding a few early post-perihelion observations to the 72 preperihelion data points reduces the barycentric orbital period by some 300 yr and its formal error by a factor of more than 20. And regardless of these errors, the orbital solutions in rows 2 to 5 of the table, whose termination observations were between Oct 28 and Nov 1, consistently display, as expected, a modest systematic trend in the predicted perihelion time and have the mean residuals measurably lower than the subsequent solutions based on longer arcs and including the later post-perihelion observations. When extrapolated from the early post-perihelion termination dates to the time of fragmentation, Oct 21.20 UT, the orbits nominally imply November 1139 for the time of comet Ikeya-Seki’s previous perihelion T_{prev} and 825.9 yr for its barycentric orbital period P_{bar} , with an error of ± 2.0 yr introduced by the extrapolation. Including the formal errors from the orbital solutions, the derived perihelion time still differs by 2σ from the time of appearance of the 1106 comet.

Starting with row 6, Table 2 provides information on the orbital solutions that include the termination dates of Nov 6, two days after the discovery of the secondary nucleus, or later. In terms of the time T_{prev} these solutions are incompatible with the four solutions in rows 2 to 5, and are more noisy, as seen from their mean residuals. The disparity in T_{prev} is clearly apparent from Figure 1. Yet, *all* values of T_{prev} in the plot deviate by one to at least three decades from the time of appearance of the 1106 comet in the same direction.

³ For comet Ikeya-Seki this time amounted to two weeks.

Table 2

Orbital Solutions for Comet Ikeya-Seki in 1965 (Epoch Oct 7.0 TT) and Time of Its Previous Perihelion Passage in the 12th Century

Termination point's time, t_{fin}		Reciprocal semimajor axis (AU^{-1})		Barycentric orbital period,	Previous perihelion,	Mean	Number	Computed
1965/66 (UT)	$t_{\text{fin}} - T$ (d)	$(1/a)_{\text{osc}}$	$(1/a)_{\text{bar}}$	P_{bar} (yr)	T_{prev}	residual	of data used ^a	offset of B from A
Oct 16.36	-4.82	$+0.007529 \pm 0.001315$	$+0.007779$	1457 ± 370	(508)	$\pm 1''.33$	72+0	...
28.35	+7.17	$+0.011002 \pm 0.000154$	$+0.011251$	837.9 ± 17.2	1127.85	± 1.37	72+2	4''/3
29.35	+8.17	$+0.010983 \pm 0.000145$	$+0.011232$	840.0 ± 16.3	1125.73	± 1.36	72+4	5.1
31.53	+10.35	$+0.010943 \pm 0.000139$	$+0.011192$	844.5 ± 15.7	1121.22	± 1.35	72+6	6.9
Nov 1.54	+11.36	$+0.010932 \pm 0.000134$	$+0.011181$	845.9 ± 15.2	1119.89	± 1.35	72+9	7.8
6.20	+16.02	$+0.011082 \pm 0.000126$	$+0.011331$	829.1 ± 13.8	1136.63	± 1.40	72+12	12.0
14.19	+24.01	$+0.011054 \pm 0.000098$	$+0.011303$	832.2 ± 10.8	1133.57	± 1.46	72+17	19.7
19.88	+29.70	$+0.010990 \pm 0.000074$	$+0.011239$	839.3 ± 8.6	1126.41	± 1.46	72+23	25.2
27.33	+37.15	$+0.010951 \pm 0.000054$	$+0.011200$	843.7 ± 6.3	1122.05	± 1.46	72+29	32.1
Dec 7.30	+47.12	$+0.010971 \pm 0.000037$	$+0.011220$	841.4 ± 4.4	1124.37	± 1.47	72+36	39.8
24.22	+64.04	$+0.010932 \pm 0.000020$	$+0.011181$	845.8 ± 2.4	1119.92	± 1.45	72+42	48.3
31.38	+71.20	$+0.010923 \pm 0.000019$	$+0.011172$	846.9 ± 2.3	1118.88	± 1.45	72+43	50.9
Jan 14.33	+85.15	$+0.010898 \pm 0.000016$	$+0.011147$	849.6 ± 1.9	1116.11	± 1.47	72+45	55.4

Note.^a Preperihelion observations + post-perihelion observations.

The formal error of the orbital period in Table 2 depends strongly on the length of the orbital arc covered by the observations. The errors from the solutions with the termination points after Nov 1 are lower than those in rows 2 to 5, even though the mean residuals vary in the opposite direction. One may question the meaning of these errors and suggest that the orbital periods and the implied perihelion times from the solutions with the termination dates of October 28 through November 1 could in fact be more accurate than they appear to be.

This argument is supported by the distribution of individual residuals listed for the orbits in rows 2–7 of Table 2 in Table 3. It is discouraging to see most of the highly consistent observations from Oct 28–Nov 1 to leave systematic residuals of $2''$ to $3''$ in right ascension from the solutions whose termination dates were after Nov 1. In fact, this trend continued to the final orbit of fragment A and was only slightly reduced by incorporating non-gravitational terms into the equations of motion.

Comparison of Marsden's (1967) relativistic set of the orbital elements for nucleus fragment A with our best gravitational and nongravitational orbits is offered in Table 4. The nongravitational solutions were computed using Style II formalism of Marsden et al. (1973). We were rather surprised that it was possible to derive the radial nongravitational parameter A_1 with a formal error as small as 20 percent. However, the value of A_1 appears to be about an order of magnitude higher than expected and it may be a product of the computing methodology, namely, the linkage of the preperihelion observations of the pre-split nucleus with the full set of the post-perihelion observations of fragment A.

We were even more surprised that we were able to derive both the radial parameter A_1 and the transverse parameter A_2 , even though the former was now determined with a higher error. The most unexpected result of this two-parameter nongravitational run was the predicted time of the previous perihelion passage, nearly 50 years after the appearance of the Great Comet of 1106. While this very late time is not necessarily very significant, it

accentuates the difficulties with the 1106 comet as Ikeya-Seki's parent.

3.2. Effects of Ikeya-Seki's Fragmentation on the Orbital Period

Intuitively, the sets of orbital elements for the two fragments into which a comet has split are plausible limits for confining the set of pre-split elements, as the fragments presumably acquired differential momenta in the opposite directions. Indeed, in implementing their two-superfragment model, Sekanina & Chodas (2004) argued that the osculating orbital period of the pre-split nucleus of comet Ikeya-Seki should have been between 880 and 1055 years (i.e., the orbital periods of the two fragments, as computed by Marsden 1967), but much closer to the first because the primary fragment should have been substantially more massive than the secondary and subjected to a much smaller effect. It so happened that by choosing the orbital period slightly longer than the period of the primary fragment, it was possible to readily link Ikeya-Seki with the 1106 comet, with an implied primary-to-secondary mass ratio of 15:1.

A view from another angle suggests that the orbital period of the pre-split comet does not have to lie between the orbital periods of the two fragments and can in fact be the shortest of the three. Let ΔP be the difference between the osculating orbital periods of the primary, A, and secondary, B, fragments of the comet at the adopted epoch of 1965 October 7.0 TT, as derived from Marsden's (1967) standard orbital solutions:

$$\Delta P = P_B - P_A = +175 \pm 5 \text{ yr.} \quad (1)$$

This result offers a total effect but says nothing about the nature of the forces that were responsible for the different motions of the two fragments. The hypothesis that it was due to an outgassing-driven differential acceleration comes from a study of the fragments' relative motion; in the orbital computations the differential acceleration is known to masquerade as an effect in the orbital period (or the eccentricity).

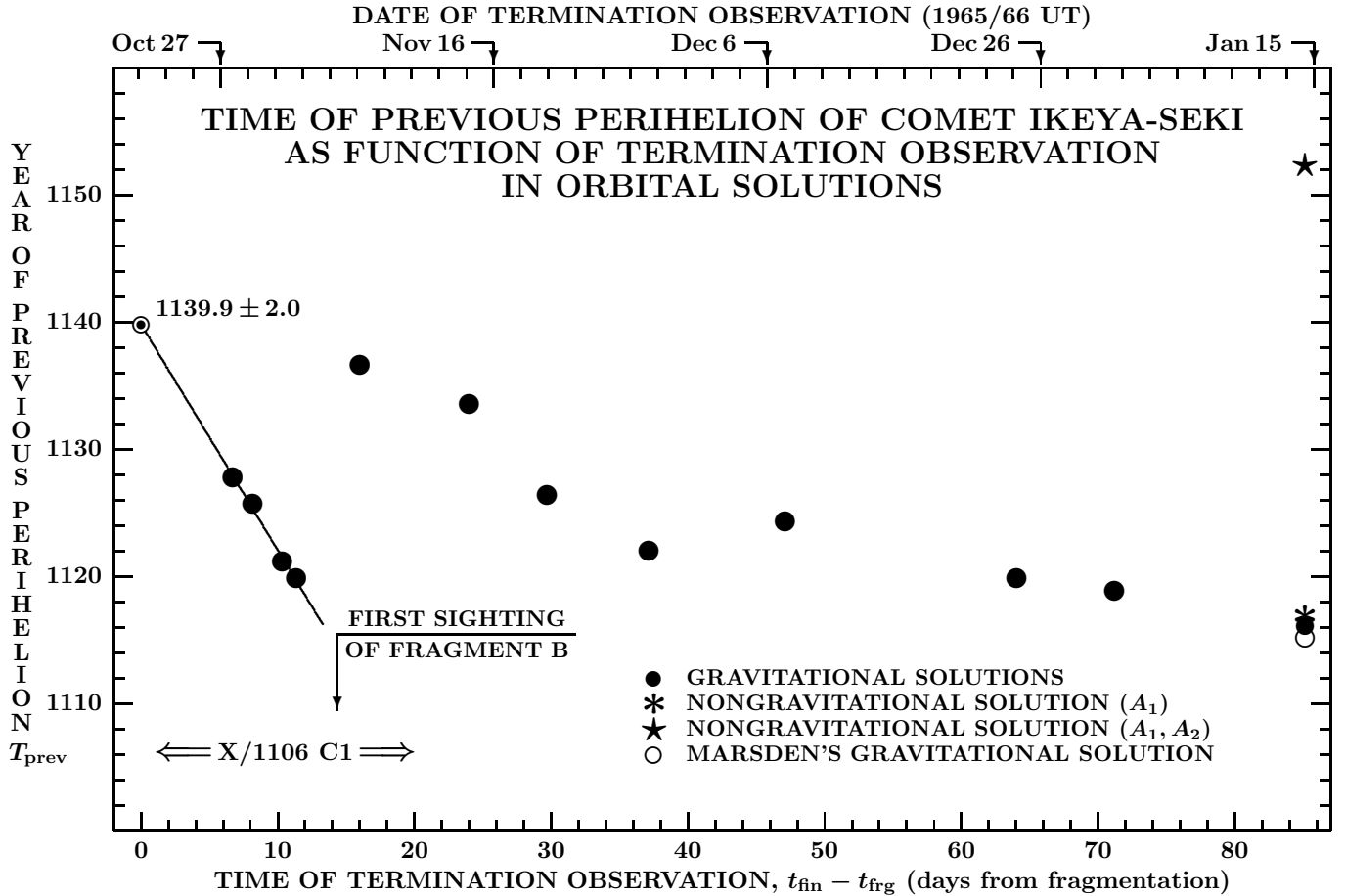


Figure 1. The time of the previous perihelion passage of comet Ikeya-Seki in the 12th century, implied by the orbital solutions with different termination points in the orbit following fragmentation. Only the early post-perihelion observations, not later than November 1 (or 12 days after perihelion), could be used as termination points to orbital solutions that offer consistent results, with the previous perihelion nominally in late AD 1139. Fragmentation appears to have taken place only a fraction of an hour after the 1965 perihelion. Note that the ordinate of not a single data point in the plot is near the time of appearance of the 1106 comet (X/1106 C1).

The motion of fragment B relative to fragment A of comet Ikeya-Seki was investigated by Sekanina (1982), using his model for the split comets. The nucleus was found to have broken up 23 ± 7 minutes after perihelion and the (radial) nongravitational acceleration was 0.67 ± 0.03 units of 10^{-5} the Sun's gravitational acceleration. The magnitude of the force, assumed to vary inversely as the square of heliocentric distance, r , was at 1 AU from the Sun equivalent to

$$\gamma = 0.20 \times 10^{-8} \text{ AU day}^{-2}. \quad (2)$$

The acceleration's contribution to the orbital velocity, V , of B relative to A, integrated over the post-fragmentation orbital arc equaled in parabolic-approximation

$$\Delta V_{\text{subl}} = \int_{t_{\text{frg}}}^{\infty} \gamma \left(\frac{r_0}{r}\right)^2 \sin \frac{1}{2}u \, dt = \frac{\gamma}{k} \sqrt{\frac{2}{r_{\text{frg}}}} r_0^2, \quad (3)$$

where t_{frg} and r_{frg} are, respectively, the fragmentation time and heliocentric distance; k the Gaussian gravitational constant, $k = 0.0172021 \text{ AU}^{\frac{3}{2}} \text{ day}^{-1}$; r_0 the unit heliocentric distance, $r_0 = 1 \text{ AU}$; and $\sin \frac{1}{2}u$ the acceleration's contribution in the direction of the orbital-velocity vector, u being the true anomaly at time t .

Because the magnitude of ΔV_{subl} is being gradually built up by the incremental contributions from the non-gravitational acceleration in the course of the apparition, only a fraction of its total is included in the value of ΔP in (1), which implies a finite upper limit of the integral in (3). This fraction is estimated to equal

$$\Delta V_{\text{subl}}^* = \Delta V_{\text{subl}} \left(1 - \sqrt{\frac{r_{\text{frg}}}{r_{\text{eff}}}}\right), \quad (4)$$

where r_{eff} is an effective heliocentric distance that describes the degree of incompleteness at which the effect is accounted for. If approximated by an average between the companion's first and last post-perihelion observations, used in the orbit determination, in terms of $r^{-\frac{1}{2}}$, it amounts to

$$r_{\text{eff}} = 4 \left(r_{\text{first}}^{-\frac{1}{2}} + r_{\text{last}}^{-\frac{1}{2}} \right)^{-2}. \quad (5)$$

With the first astrometric observation of fragment B on 1965 Nov 12.8 and its last observation on 1966 Jan 14.3 UT, we have $r_{\text{first}} = 0.87 \text{ AU}$, $r_{\text{last}} = 2.12 \text{ AU}$, $r_{\text{eff}} = 1.29 \text{ AU}$, and

$$\Delta V_{\text{subl}}^* = 0.92 \Delta V_{\text{subl}}. \quad (6)$$

Table 3
Residuals of Post-Perihelion Observations of Comet Ikeya-Seki from Six of the Orbital Runs in Table 2

Time of observation 1965 (UT)	Sept 21–Nov 14		Sept 21–Nov 6		Sept 21–Nov 1		Sept 21–Oct 31		Sept 21–Oct 29		Sept 21–Oct 28	
	(<i>o-c</i>) _{RA}	(<i>o-c</i>) _{Dec}	(<i>o-c</i>) _{RA}	(<i>o-c</i>) _{Dec}	(<i>o-c</i>) _{RA}	(<i>o-c</i>) _{Dec}	(<i>o-c</i>) _{RA}	(<i>o-c</i>) _{Dec}	(<i>o-c</i>) _{RA}	(<i>o-c</i>) _{Dec}	(<i>o-c</i>) _{RA}	(<i>o-c</i>) _{Dec}
Oct 28.34795	+0 ^{''} .2	−1 ^{''} .0	−0 ^{''} .5	−0 ^{''} .7	−0 ^{''} .9	−1 ^{''} .0	−1 ^{''} .5	−0 ^{''} .8	−1 ^{''} .2	−0 ^{''} .4	−0 ^{''} .3	+0 ^{''} .3
28.35182	+1.6	−1.1	+1.0	−0.8	+0.5	−1.1	−0.1	−0.9	+0.3	−0.5	+1.1	+0.1
29.34461	+2.4	+0.4	+1.6	+0.7	+1.0	+0.3	+0.4	+0.5	+0.8	+1.0
29.34938	+2.5	−0.3	+1.8	0.0	+1.2	−0.4	+0.5	−0.2	+0.9	+0.3
31.53131	+3.2	+0.8	+2.2	+1.1	+1.4	+0.5	+0.6	+0.6
31.53304	+3.3	+1.0	+2.4	+1.4	+1.5	+0.7	+0.7	+0.9
Nov 1.11825	−0.8	+0.8	−1.8	+1.1	−2.7	+0.4
1.53440	+1.6	+1.1	+0.5	+1.4	−0.4	+0.7
1.53544	+1.4	+0.1	+0.3	+0.4	−0.6	−0.4
5.10799	−0.4	+0.7	−1.8	+1.0
5.12985	+0.7	−2.2	−0.7	−1.9
6.19913	−0.8	−2.7	−2.3	−2.4
8.19913	−2.2	−1.8
9.89120	(−5.3	+0.4)
10.13946	−2.4	+3.3
11.34018	(−5.3	−0.8)
12.83588	−0.6	+1.0
14.09479	(−6.2	+2.1)
14.09479	−2.7	+0.3
14.18647	−0.2	−0.2

In near-parabolic approximation, a change of ΔV in the orbital velocity implies a change of ΔP in the orbital period that equals generally

$$\Delta P = \kappa P^{\frac{5}{3}} r_{\text{frg}}^{-\frac{1}{2}} \Delta V, \quad (7)$$

where

$$\kappa = 3(\sqrt{2}k\pi^2)^{-\frac{1}{3}}. \quad (8)$$

Inserting (3), (4), and (8) into (7), we obtain for ΔP_{subl} , the part of the difference between the orbital periods of the two fragments caused by the sublimation,

$$\Delta P_{\text{subl}} = 3 \left(\frac{\sqrt{2}}{\pi k^2} \right)^{\frac{2}{3}} P^{\frac{5}{3}} \frac{\gamma r_0^2}{r_{\text{frg}}} \left(1 - \sqrt{\frac{r_{\text{frg}}}{r_{\text{eff}}}} \right). \quad (9)$$

Inserting next the value of γ from (2), $P = 880$ yr, and $r_{\text{frg}} = 0.00807$ AU, one gets

$$\Delta P_{\text{subl}} = 373 \text{ yr}, \quad (10)$$

a result that is very different from ΔP in (1). This means that the difference between the fragments' orbital periods was *not* caused by the outgassing effect *alone*.

The other effect is schematically shown in Figure 2, which depicts an irregularly shaped nucleus very shortly before and after it split tidally in two along a section approximately perpendicular to the radius vector. The breakup is most likely to occur when the longest dimension of the nucleus is aligned with the direction to the Sun, as the tidal effect reaches then a maximum. The nucleus is broken up in one of two possible ways: the primary, more massive fragment A ends up on the sunward side, or on the antisunward side. At the moment of the breakup, both fragments have the same orbital velocity, but their centers of mass are at uneven heliocentric

distances, whose difference equals the distance between their centers of mass. As a result, the two fragments begin to move in different orbits, with absolutely *no momentum exchange* involved. Differentiating the expression for the orbital velocity V , we have at fragmentation:

$$2VdV = k^2 \left(a^{-2} da - 2r_{\text{frg}}^{-2} dr \right), \quad (11)$$

where a is the semimajor axis of the pre-split comet, da is the difference between the semimajor axes of the separated fragments, and dr is the difference between the heliocentric distances of the fragments' centers of mass. Differentiating the relationship between the semimajor axis and the orbital period, we have

$$da = \frac{2}{3} (k/2\pi)^{\frac{2}{3}} P^{-\frac{1}{3}} dP. \quad (12)$$

Next, we note that dr in (11) equals ℓ , the difference in the distance from the Sun between the centers of mass at the time of the breakup, in the sense fragment B minus fragment A and, similarly, dP in (12) equals ΔP_{sep} , the difference in the fragments' orbital periods triggered by this finite separation distance ℓ , also in the sense fragment B minus fragment A. Since $dV = 0$ in (11), we get for ℓ by inserting from (12) into (11)

$$\ell = \frac{1}{3} (2\pi/k)^{\frac{2}{3}} P^{-\frac{5}{3}} r_{\text{frg}}^2 \Delta P_{\text{sep}}. \quad (13)$$

This relation means that when the secondary fragment is farther from the Sun at breakup ($\ell > 0$), it is injected, by this virtue alone, into an orbit of longer period than the primary fragment as shown in Scenario I in Figure 2, and vice versa.

We now propose that the two effects, one driven by the outgassing, ΔP_{subl} , and given by (9), *plus* the other, triggered by the radial separation of the fragments' centers

Table 4

Comparison of Marsden's and This Study's Relativistic Orbital Elements for Nucleus A of Comet Ikeya-Seki (C/1965 S1) (Equinox J2000; Osculation Epoch 1965 Oct 7.0 TT)

Orbital element	Orbital solution by Marsden (1967)	Orbital solutions in this study		
		gravitational	nongravitational, A_1	nongravitational, $A_1 + A_2$
Perihelion time, T , 1965 Oct (TT)	21.183679 ± 0.000049	21.183661 ± 0.000053	21.183541 ± 0.000084	21.183635 ± 0.000101
Argument of perihelion, ω	$69^\circ 04862 \pm 0^\circ 00048$	$69^\circ 04902 \pm 0^\circ 00046$	$69^\circ 05143 \pm 0^\circ 00064$	$69^\circ 05446 \pm 0^\circ 00112$
Longitude of ascending node, Ω	$346^\circ 99467 \pm 0^\circ 00060$	$346^\circ 99501 \pm 0^\circ 00057$	$346^\circ 99289 \pm 0^\circ 00070$	$346^\circ 99766 \pm 0^\circ 00158$
Orbit inclination, i	$141^\circ 86415 \pm 0^\circ 00014$	$141^\circ 86430 \pm 0^\circ 00014$	$141^\circ 86415 \pm 0^\circ 00013$	$141^\circ 86512 \pm 0^\circ 00032$
Perihelion distance, q (AU)	$0.00778572 \pm 0.00000020$	$0.00778593 \pm 0.00000021$	$0.00778124 \pm 0.00000098$	$0.00778568 \pm 0.00000163$
Orbit eccentricity, e	$0.99991521 \pm 0.00000013$	$0.99991515 \pm 0.00000013$	$0.99991416 \pm 0.00000014$	$0.99991206 \pm 0.00000073$
Reciprocal semimajor axis, $1/a$ (AU $^{-1}$)	$+0.010891 \pm 0.000017$	$+0.010898 \pm 0.000016$	$+0.011031 \pm 0.000019$	$+0.011295 \pm 0.000092$
Orbital period, P (yr)	879.9 ± 2.1	878.9 ± 2.0	863.1 ± 2.2	833.0 ± 10.3
Nongravitational parameters:				
A_1 (10^{-8} AU day $^{-2}$)	$+1.86 \pm 0.38$	$+0.96 \pm 0.46$
A_2 (10^{-8} AU day $^{-2}$)	$+0.0074 \pm 0.0022$
Mean residual	$\pm 1''.2$	$\pm 1''.47$	$\pm 1''.40$	$\pm 1''.37$
Number of data used (pre+post)	75+44	72+45	72+45	72+45
Predicted year of previous perihelion	1115.2	1116.11	1116.17	1152.36

of mass at breakup, ΔP_{sep} , and given by (13), should, when added together, result in the difference in the orbital period, ΔP , ascertained from the standard orbital solutions for the fragments and given by (1):

$$\Delta P_{\text{subl}} + \Delta P_{\text{sep}} = \Delta P. \quad (14)$$

This condition gives for Ikeya-Seki

$$\Delta P_{\text{sep}} = 175 - 373 = -198 \text{ yr} \quad (15)$$

and implies that, from (13), the separation between the two fragments' centers of mass equaled

$$\ell = -8.0 \text{ km}. \quad (16)$$

Being negative, the distance ℓ fits Scenario II in Figure 2: the secondary fragment, B, was at the time of breakup at the sunward end of the parent nucleus. It is further apparent from Figure 2 that the center of mass of the pre-split comet was also sunward of the center of mass of the primary fragment and that therefore the pre-split comet moved in an orbit of *shorter period than the primary nucleus*. In addition, of course, it is very likely that the primary fragment was subjected to a higher nongravitational acceleration than the parent nucleus, which should increase the difference in their orbital periods further. The purpose of this exercise was to call attention to an effect involving the center of mass of fragments in events of tidal disruption and allowing one to offer limited information on the fragments' sizes, which we comment on in Section 3.3.

Using the differentiation was very convenient, but made the results approximate especially because the differences were relatively large. For example, an expression for ℓ more accurate than (13) is

$$\ell = \frac{1}{2} \left(\frac{2\pi}{k} \right)^{\frac{2}{3}} r_{\text{frg}}^2 \left(P_A^{-\frac{2}{3}} - P_B^{-\frac{2}{3}} \right). \quad (17)$$

As a word of caution, we note that reports of additional, temporary fragments may suggest other possible explanations for the short orbital period of the pre-split

comet Ikeya-Seki, not necessarily negating a momentum-exchange effect. Hirayama & Moriyama (1965) reported that only minutes after perihelion they observed coronagraphically the comets' head splitting into three components, one of them being much brighter than the other two. We believe that this event was not the one giving birth to fragment B. Independently, Pohn (1965) remarked on a potential third nucleus on November 4.5 UT, while Andrews (1965) noted that on November 6.1 UT the secondary nucleus was possibly a triple complex. It is beyond the scope of this paper to judge the potential influence of these transient phenomena on the orbit of the pre-split nucleus, and we limit ourselves to merely mentioning them for the benefit of the reader.

3.3. The Ramifications

In Section 3.1 we argued that before splitting at its 1965 perihelion, comet Ikeya-Seki was moving in an orbit of a period that was shorter than that of either fragment. The comet's previous return to perihelion was thus found to have occurred decades after the appearance of the Great Comet of 1106, most probably near the year 1139, and offering strong evidence for ruling out the 1106 comet as Ikeya-Seki's parent and previous appearance. And because there is no doubt that the Great September Comet of 1882 and Ikeya-Seki were on their approach to their previous perihelion a single object, our result rules out an association between the comets of 1106 and 1882 as well.

In Section 3.2 we showed that it is dynamically feasible for a sungrazer, prior to its breaking up tidally in close proximity of perihelion, to move in an orbit with a shorter period than that of either of its two nuclear fragments, thereby corroborating the results of Section 3.1. This problem deserves further attention in the future.

The probable time of the previous perihelion return of Ikeya-Seki around the year 1139 opens two questions: one is the role of the Great Comet of 1106 in the history of the Kreutz system, the other is the whereabouts of the parent to Ikeya-Seki and the 1882 comet. The first ques-

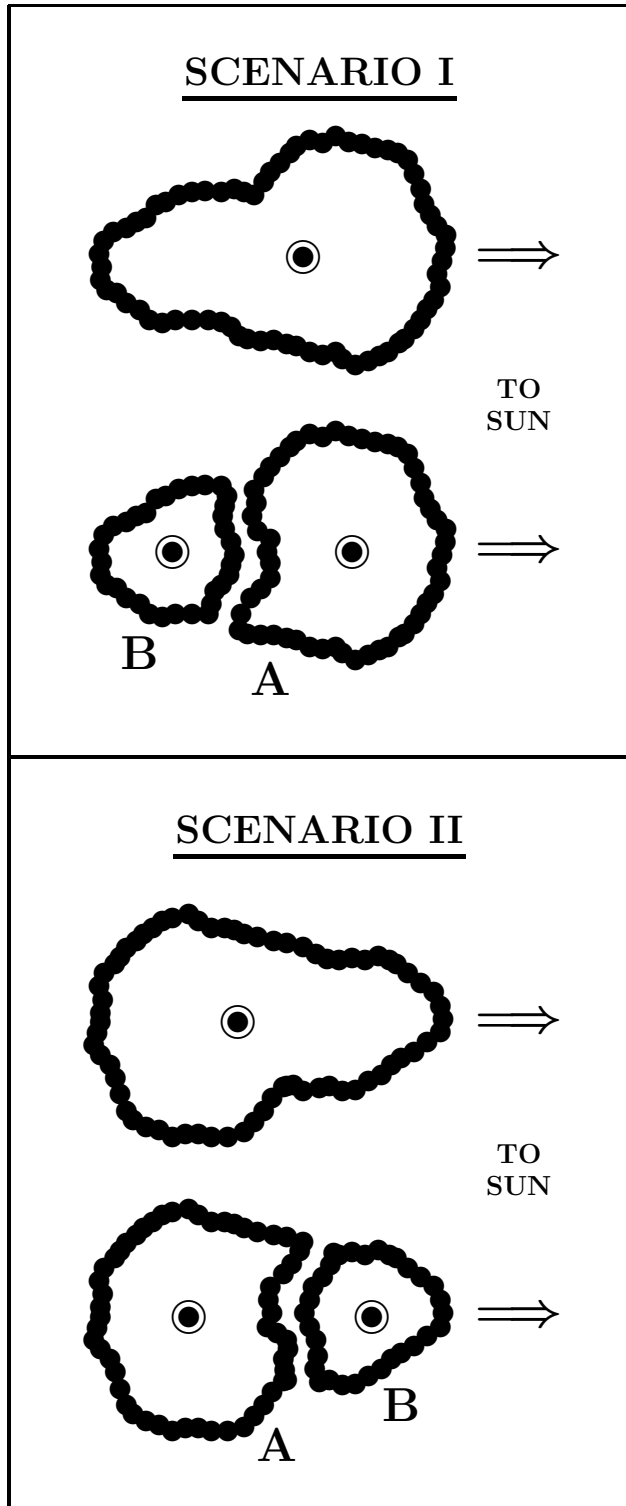


Figure 2. Elongated cometary nucleus of a sungrazing comet shortly before and after breaking up tidally into two uneven fragments at perihelion. Turned to the Sun (to the right) at the time of breakup is the larger end of the nucleus, to become the primary fragment A, in Scenario I, but the smaller end, to become the secondary fragment B, in Scenario II. The large circled dots are the positions of the centers of mass of the parent (or pre-split) nucleus, at the top of either panel, and of the fragments A and B at the bottom. Accordingly, the orientation relative to the Sun alone assures that fragment A ends up in an orbit of a shorter period and fragment B in an orbit of a longer period than was the parent in Scenario I, whereas the opposite is true in Scenario II.

tion was addressed in part by Sekanina & Chodas (2008), when they concluded that the orbit for the Great March Comet of 1843 derived from the best available astrometric observations did not rule out its previous return to perihelion as the Great Comet of 1106.

The two giant sungrazers of the 19th century, the Great March Comet of 1843 and the Great September Comet of 1882, moving in orbits similar but not nearly identical and representing two major populations of the Kreutz system, implied the existence of two major sungrazers in the first half of the 12th century, given that their barycentric orbital periods were close to 750 years.⁴ Yet, no candidate other than the 1106 comet has ever been seriously proposed. The solution to this problem was usually circumvented by pointing out that a sungrazer arriving at perihelion between late May and early August approaches from behind the Sun and recedes in that same direction, thus being missed unless it is bright enough to be seen in broad daylight. Closer inspection of relevant circumstances shows that this is not necessarily so, but it is true that such a sungrazer could at best be detected as an unimpressive naked-eye object whose record in historical annals would be far less notable than that of the 1106 comet.

We did not undertake a concerted effort in search for the “missing” sungrazer, but merely conducted a cursory perusal of Ho’s (1962) catalogue of the ancient and medieval observations of comets in the Far East. Under the entry 403 we came across brief descriptions of two obviously different objects from late August and September 1138, one Japanese, the other Chinese. The Japanese object was of no interest, but the text on the Chinese comet caught our attention. The primary source was the 29th volume of *Sung Shih*, a historical account of the Sung Dynasty compiled from older sources in 1345, and the secondary source was the 14th volume of *Hsü Thung Chien Kang Mu*. The relevant record for 1138 says:

On September 3 a broom star (hui) was observed in the east. It went out of sight on September 29.

The used terminology (hui) suggests that the comet had a tail (even though its length was not given) and, while not explicitly stated, the comet must have been seen in the morning sky, before sunrise.

This Chinese comet of 1138 is neither among the Kreutz candidates proposed by Hasegawa & Nakano (2001) nor on England’s (2002) list of possible early Kreutz sungrazers. Hasegawa’s (1980) catalogue contains this object under the entry number 636 and notes that it also was included in the compilations by Pingré (1783) and by Kanda (1935). The circumstances at the time of appearance of this possible major sungrazer are examined in some detail in Section 4.

We call attention to a case of remarkable coincidence, as Marsden’s (1967) integration of Kreutz’s (1888, 1891)

⁴ Unfortunate was the lingering belief that the orbital period of the 1843 sungrazer was much shorter, near 500 yr, predicated on the earlier results by Kreutz (1901) and by Hubbard (1852) before him, while still others (e.g., Nicolai 1843) noted that the choice of the orbital period made almost no difference in the representation of observations. The modern revision, with a period longer than 700 yr deemed feasible, had been unavailable until fairly recently (Sekanina & Chodas 2008).

nonrelativistic orbit of the brightest fragment B (No. 2 in Kreutz’s notation) of the Great Comet of 1882 back in time gave the previous perihelion passage in April 1138, only months before arrival of the proposed Kreutz candidate.⁵ The center of mass of fragment B was apparently slightly sunward of the center of mass of the 1882 parent comet at the time of its perihelion fragmentation, which together with a contribution from the differential outgassing-driven nongravitational acceleration could provide a near-zero effect in the orbital period between the parent and fragment B. If so, the times of the previous perihelion for nucleus fragment B and the parent comet should be about the same and the amazing agreement of Marsden’s prediction with the timing of the 1138 comet may not be fortuitous.

The data on the fragmentation of Ikeya-Seki offer limited information on the size of the comet’s nucleus. In a first approximation, the distance of 8 km between the centers of mass of the two fragments in (16) equals the semidiameter of the long axis of the pre-split nucleus. If the axial ratios are, for example, 1:1:2, the effective diameter of the pre-split nucleus is 10 km. If the comet of 1138 is indeed the previous appearance of Ikeya-Seki, the difference between the orbital periods of nuclear fragment A (our gravitational or A_1 nongravitational solution) and the pre-split comet is about 22 yr. Interpreted in its entirety as an effect of separation at fragmentation (rather than a sublimation effect), it offers a lower limit to the fragment A-to-fragment B mass ratio equaling 8, equivalent to a lower limit of 2 for the fragment A-to-fragment B size ratio. The effective diameters of fragments A and B then come out to be about 9.6 km and 4.8 km, respectively.

4. THE CHINESE COMET OF 1138

Even though the description of the Chinese comet of 1138 in Ho’s (1962) catalogue is brief, important insights into the issue of the object’s association with the Kreutz system can be gained. We approximate the angular elements and perihelion distance of the orbit of the 1138 comet by the values originally derived for the presumed 1106 apparition of the Great September Comet of 1882 (Sekanina & Chodas 2002), assume the orbit to be a parabola, and address the membership issue in some detail in the following.

4.1. Observing Site

To examine the observing conditions, we need to have an idea on the geographic location of the probable observing site. The (southern) Sung Dynasty’s capital was Jiangning (today a southern district of Nanjing, the capital of Jiangsu Province) until 1138 and Lin’an (nowadays a district of Hangzhou, the capital of Zhejiang Province) from 1138 on.⁶ The distance between the two cities, where information on the comet’s sightings was presumably coming from, is only about 200 km and their loca-

tions can approximately be depicted by geographic longitude 120° east of Greenwich, latitude 31° north of the equator, and 20 meters above sea level. The observing window up to sunrise on September 3, between 4:00 and 5:40 local time, is equivalent to Sept 2.83–2.90 UT.

4.2. Limiting Magnitude

Before addressing the issue of light curve of the 1138 comet, we examined the observing conditions during the critical period of time in the morning of September 3, the day of the first recorded sighting, and September 29, the day of disappearance. The conditions for detecting, with the unaided eye, a stellar object of apparent visual magnitude H_{app} at a given location of the sky from a given observing site are described by a limiting magnitude, H_{lim} , determined from an algorithm developed by Schaefer (1993, 1998) as a function of (i) the object’s solar and lunar elongations; (ii) the object’s, Sun’s, and Moon’s elevations above the local horizon, and the Moon’s phase; and (iii) the atmospheric and other conditions at the observing site. The algorithm also allows for seasonal and long-term effects. In a recent paper, Sekanina (2022; referred to hereafter as Paper 2) employed the Schaefer algorithm, strictly valid for stellar objects, to comets. By introducing and applying a *visibility index* \mathfrak{S} ,

$$\mathfrak{S} = H_{\text{lim}} - H_{\text{app}}, \quad (18)$$

he found meaningful results when tested on daylight magnitude estimates of the sungrazing comet Ikeya-Seki in October 1965. The more positive the value of \mathfrak{S} is, the better prospect there is to detect, with the naked eye, a comet of magnitude H_{app} at a location of the sky at which the limiting magnitude is H_{lim} . A value of \mathfrak{S} near zero, within a few tenths of a magnitude, means a marginal chance of seeing the object or the point of disappearance.

Moonlight interfered with observation of the 1138 comet on both September 3 and September 29. The new moon was on September 6.29 UT and October 5.96 UT. We adopted an obvious view that because disappearing 26 days after the first sighting the comet was during September gradually fading and therefore receding from the Sun, having passed perihelion before September.

An estimate of the perihelion time was a key parameter for investigating the comet as a potential Kreutz sungrazer. A crude guess was obtained by straightforwardly comparing the 1138 comet to comet Pereyra (C/1963 R1), a definite member of the Kreutz system discovered on 1963 September 14 and passing perihelion 21 days earlier. By simply shifting the dates, the perihelion passage of the 1138 comet was predicted to have taken place on August 13. In spite of the vastly different circumstances at the two comets’ arrival times more than 800 years apart, this guess eventually turned out to be not too far off the mark, to the extent we can judge.

Based on this guess, we selected three candidate dates — July 23, August 1, and August 10 — for the 1138 perihelion time. For the observing site defined in Section 4.1 and the dates of 1138 September 3 and 29 we computed, for a number of times (between the comet’s rise above the eastern horizon and sunrise) at a step of 18 minutes, the horizontal coordinates (the azimuth reckoned from the south clockwise) of the Sun, the Moon, and

⁵ The relativistic orbit of fragment B of the 1882 comet was computed by Hufnagel (1919), who derived a period shorter than the period of Kreutz’s nonrelativistic orbit by more than 10 yr. This large difference makes Hufnagel’s result, which according to Marsden (1967) implies November 1149 for the time of the previous perihelion passage of the 1882 comet, rather suspect.

⁶ The northern territories of the Sung Dynasty were lost to the Jin Dynasty in 1127.

Table 5Predicted Path of Comet 1138 and the Limiting Magnitude H_{lim} on 1138 September 3 As Function of Perihelion Date

Local time	Elevation		Perihelion: 1138 July 23			Perihelion: 1138 August 1			Perihelion: 1138 August 10		
	Sun	Moon	Azimuth	Elevation	H_{lim}	Azimuth	Elevation	H_{lim}	Azimuth	Elevation	H_{lim}
3:57	-22°1	+12°7	-82°5	+6°0	3.6	-85°0	+3°5	2.2	-88°3	+0°1	-8.6
4:15	-18.5	+16.4	-80.0	+9.8	4.4	-82.6	+7.3	3.7	-86.0	+4.0	2.4
4:33	-14.8	+20.1	-77.6	+13.6	3.6	-80.2	+11.1	3.4	-83.6	+7.9	2.4
4:51	-11.1	+23.9	-75.0	+17.3	3.0	-77.7	+14.9	2.8	-81.2	+11.7	2.4
5:09	-7.3	+27.6	-72.3	+21.0	2.2	-75.1	+18.7	2.0	-78.7	+15.5	1.7
5:27	-3.5	+31.4	-69.4	+24.7	0.0	-72.4	+22.4	-0.2	-76.1	+19.3	-0.6
5:45	+0.3	+35.1	-66.4	+28.3	-3.2	-69.5	+26.0	-3.5	-73.4	+23.0	-3.8

Table 6Predicted Path of Comet 1138 and the Limiting Magnitude H_{lim} on 1138 September 29 As Function of Perihelion Date

Local time	Elevation		Perihelion: 1138 July 23			Perihelion: 1138 August 1			Perihelion: 1138 August 10		
	Sun	Moon	Azimuth	Elevation	H_{lim}	Azimuth	Elevation	H_{lim}	Azimuth	Elevation	H_{lim}
2:27	-44°4	+30°9	-74°2	+5°1	1.4	-75°8	+2°9	-0.4	-77°7	+0°3	-8.7
3:03	-37.4	+38.4	-69.2	+12.5	3.3	-70.9	+10.3	3.0	-72.9	+7.8	2.5
3:39	-30.0	+45.9	-63.6	+19.5	4.0	-65.5	+17.5	3.8	-67.7	+15.0	3.6
4:15	-22.4	+53.3	-57.4	+26.3	4.3	-59.5	+24.4	4.3	-61.9	+22.0	4.2
4:51	-14.8	+60.4	-50.2	+32.5	4.3	-52.5	+30.8	4.2	-55.4	+28.7	4.2
5:27	-7.0	+67.0	-41.6	+38.1	2.9	-44.5	+36.6	2.8	-47.7	+34.7	2.7
6:03	+0.7	+72.4	-31.7	+42.7	-2.5	-35.0	+41.5	-2.6	-38.7	+40.0	-2.7

the comet on each of the three perihelion-time assumptions, and derived the limiting magnitudes as a function of time. On September 3 the comet was found to have risen between 3:43 and 3:57 local time (19:43 to 19:57 UT on September 2) as the perihelion time advanced from July 23 to August 10, while sunrise occurred on 5:43 local time (21:43 UT on September 2). This means that the comet could be observed for quite a bit less than two hours in early September. On September 29 the comet could be seen over three hours, so that the more restrictive viewing conditions on September 3 offered tighter constraints on the perihelion time.

The quantities that varied during observation are presented in Table 5 for the morning hours of September 3 and in Table 6 for September 29, while the other positional data on the comet, the Sun, and the Moon on

Table 7

Positional Data on the Comet of 1138, the Sun, and the Moon in the Mornings of 1138 September 3 and 29

Observation time, 1138 (local time)	Date of perihelion 1138 (0 TT)	Distance (AU) from		Elongation	
		Sun	Earth	solar	lunar
Sept 3.2	Jul 23	1.32	1.92	40°0	16°4
	Aug 1	1.12	1.76	36.4	15.5
	Aug 10	0.90	1.59	31.7	15.4
Sept 29.2	Jul 23	1.82	2.05	62.8	30.1
	Aug 1	1.66	1.91	60.1	31.2
	Aug 10	1.48	1.71	56.9	32.8

September 3 and 29 as a function of the comet's assumed perihelion time are listed in Table 7. The comet's azimuths in Table 5 show that the condition of the comet appearing on September 3 in the east was closely satisfied; at elevation 12°, for example, to 9° if perihelion occurred on August 10, to better than 12° if on August 1, and to better than 13° if on July 23.

The curves of the limiting magnitude in Tables 5 and 6 are U-shaped. On September 3 the bright ends reflect, respectively, the high atmospheric extinction as the comet rose above the horizon before 4:00, and the dawn effect before sunrise a minute or so before 5:45. Only before about 4:30 is the limiting magnitude on either date affected significantly by moonlight. The comet should have been the fainter — but also the sooner above the horizon — the earlier it passed through perihelion. The brightness effect favors a later perihelion passage, the horizon-crossing effect an earlier one. Perihelion on August 10 would require the comet to have been of magnitude 1–2 or brighter on September 3. An important conclusion from Table 6 is that the comet should have been close to magnitude 4.2–4.3 on September 29 regardless of the perihelion time, given its disappearance on that day. Combined with a brightness estimate on September 3, based on the limiting magnitudes in Table 5, the assumption of August 10 perihelion implies that the comet should have faded steeply with heliocentric distance r , more steeply in fact than r^{-4} , otherwise it could be seen on September 3 for only a short period of time at very low elevations. These arguments suggest that the comet's perihelion passage occurred with high probability *before* August 10.

Table 8
Observing Conditions During September 1138 at Midpoint of Astronomical Twilight (Perihelion on August 1.0 TT)

Date 1138	Local time	Distance (AU) from		Elongation		Moon's eleva- tion	Fraction of Moon's disk illuminated	Midpoint of astronomical twilight				
		Sun	Earth	solar	lunar			Azim.	Elev.	H_{lim}	H_{app}	\Im
Sept 3	4:33	1.12	1.76	36°4	15°5	+20°1	0.11	-80°2	+11°1	3.2	2.4	+0.8
6	4:35	1.19	1.79	39.0	33.4	-11.8	0.00	-77.4	+13.5	3.7	2.6	+1.1
9	4:37	1.25	1.81	41.7	67.2	-44.4	0.07	-74.6	+15.9	4.0	2.9	+1.1
12	4:39	1.32	1.83	44.4	103.2	-75.2	0.29	-71.7	+18.3	4.3	3.1	+1.2
15	4:41	1.38	1.85	47.1	140.0	-60.5	0.60	-68.6	+20.6	4.5	3.3	+1.2
18	4:43	1.44	1.87	49.9	159.3	-22.0	0.89	-65.5	+22.9	4.7	3.5	+1.2
21	4:45	1.50	1.88	52.6	125.7	+18.8	1.00	-62.2	+25.1	3.4	3.7	-0.3
25	4:48	1.58	1.90	56.4	73.5	+68.3	0.78	-57.6	+28.0	4.0	3.9	+0.1
29	4:51	1.66	1.91	60.1	31.2	+60.4	0.40	-52.5	+30.8	4.2	4.1	+0.1

We further note that a sungrazer of apparent magnitude 4.2–4.3 six weeks after perihelion — the scenario with perihelion on July 23 — implies an intrinsically very bright comet. Such a comet should have been sighted sooner at a smaller solar elongation than 40° (Table 7). It is improbable that perihelion took place as early as July 23. While the exact date of perihelion remains unknown, we find it most likely that the comet passed perihelion within several days of August 1. Below we adopt the Chinese comet of 1138 as the presumed parent to the Great September Comet of 1882 and comet Ikeya-Seki, and August 1 as the date of its perihelion passage.

In Table 8 we present an ephemeris of the 1138 comet, assuming perihelion on August 1.0 TT. The ephemeris is short in terms of the number of entries, which are the midpoints of astronomical twilight (with the Sun $\sim 15^\circ$ below the horizon), but it is extended in terms of the number of listed quantities. The table allows one to acknowledge that, of the nine listed dates, moonlight was disturbing on four. The interference on September 21, just hours after the full moon was so strong that the comet may have been lost only to be marginally detected again before its ultimate disappearance, to which moonlight also contributed its share. The final two columns of Table 8 will be commented on in the next section.

4.3. Light Curve of the Comet of 1138

In the absence of any direct information, we turn for help to Paper 2, in which the problem of sungrazers' light curves was discussed in broad terms. A comet's visual brightness was investigated using the usual power-law formula, which on a magnitude scale is

$$H_{\text{app}}(r, \Delta; H_0, n) = H_0 + 2.5n \log r + 5 \log \Delta, \quad (19)$$

where $r = r(t)$ is the heliocentric distance and $\Delta = \Delta(t)$ the geocentric distance (both in AU) of the comet at the time of observation, t ; H_0 is the absolute magnitude (normalized to $r = \Delta = 1$ AU); and n is a photometric exponent equal to the power of heliocentric distance with which the brightness, normalized to a unit geocentric distance, inversely varies, r^{-n} . Since the light curves of major Kreutz sungrazers are known to be, in general, asymmetric relative to perihelion, the preperihelion parameters, H_0^- , n^- , and the post-perihelion parameters, H_0^+ , n^+ were examined in Paper 2 separately. The

preperihelion photometric exponents of all major Kreutz sungrazers were assumed to be constant⁷ and equal to $n^- = 4$, while the post-perihelion photometric exponents were deemed a function of perihelion fragmentation. For a sungrazer with the nucleus breaking up at perihelion into N_{frg} fragments, the post-perihelion value of the exponent was adopted to vary as

$$n^+ = 4.4 - 0.2N_{\text{frg}}, \quad (20)$$

where $N_{\text{frg}} = 1$ when the comet does not fragment. This equation expresses the well-known fact that major sungrazers fade rather rapidly, unless they break into persisting fragments at perihelion. This empirical relationship is based on an extensive amount of data on comet Ikeya-Seki, a modest set of data on the Great September Comet of 1882, and fragmentary data on the Great March Comet of 1843, collected in Paper 2. The preperihelion absolute magnitudes H_0^- were estimated at 5.9 for Ikeya-Seki, 3.4 for the 1882 sungrazer, and 3.5 for the 1843 sungrazer. The post-perihelion absolute magnitude H_0^+ was linked to the preperihelion value by requiring perihelion continuity,

$$H_0^- + 2.5n^- \log q + 5 \log \Delta_q = H_0^+ + 2.5n^+ \log q + 5 \log \Delta_q, \quad (21)$$

where q is the perihelion distance and Δ_q the geocentric distance of the comet at perihelion (both in AU). With $n^- = 4$ and n^+ from (20), the post-perihelion absolute magnitude was found to equal

$$H_0^+ = H_0^- - (1 - \frac{1}{2}N_{\text{frg}}) \log q. \quad (22)$$

The post-perihelion photometric exponent amounted to 4.0 for comet Ikeya-Seki ($N_{\text{frg}} = 2$), 3.3 for the 1882 comet (assuming $N_{\text{frg}} = 5$ to 6), and 4.2 for the 1843 comet ($N_{\text{frg}} = 1$). From (22) the post-perihelion absolute magnitude came out to be 5.9 for Ikeya-Seki, -0.2 for the 1882 comet, and 4.6 for the 1843 comet. The parent sungrazers were arbitrarily assigned in Paper 2 the preperihelion absolute magnitudes 0.6 mag brighter than their primary fragments (the 1843 and 1882 comets). We now recognize the comet of 1138 as one of the two parents.

⁷ This approximate rule does under no circumstances apply to the SOHO Kreutz sungrazers.

The number of fragments into which the 1138 comet broke up is of course unknown, but it could not be smaller than two — the 1882 comet and Ikeya-Seki. Potentially, the comet may also be a parent to Strom’s (2002) sun-comet of 1792 as well as to the probable sungrazer X/1702 D1 (Kreutz 1901; Marsden 1967); that would make the number of the persistent fragments equal four. We can only speculate whether another major fragment might arrive in the coming decades. If we accept that the nucleus of the 1138 comet split at perihelion into the four pieces, then its light-curve parameters $n^+ = 3.6$ and $H_0^+ = 0.7$ (assuming that $H_0^- = 2.8$ or 0.6 mag brighter than H_0^- for the 1882 comet). The post-perihelion light curve then follows the formula

$$H_{\text{app}} = 0.7 + 9 \log r + 5 \log \Delta. \quad (23)$$

The ephemeris in Table 8 provides the apparent magnitudes from this formula in the penultimate column. The table’s last column offers the values for the visibility index of the comet at the midpoint of astronomical twilight. One can see that for more than two weeks after September 3 the computed magnitude was compatible with the comet’s visibility with the unaided eye. The situation worsened suddenly with the arrival of the full moon on September 21, when the predicted visual perception of the comet apparently indicated it dropped below the detection threshold. Toward the end of the month the interference by moonlight subsided a little, but the comet grew gradually fainter until eventually vanishing, as the limiting magnitude after September 29 remained essentially constant.

The tabulated values of the visibility index \mathfrak{S} were computed assuming constant atmospheric conditions, an assumption that is unavoidable but in practice never satisfied. For example, the observing conditions deteriorate as air humidity climbs; an increase from 50 percent to 80 percent can cause the visibility limit can shoot up by 0.5 mag or more. A few days with higher humidity beginning on September 29 may have been all that was needed for this date to be recorded as the point of disappearance.⁸

Our last item on the light curve proposed for the 1138 comet is a plot of the apparent magnitude against the solar elongation when the brightness variation with heliocentric distance follows the law (23) after perihelion and the corresponding law ($H_0^- = 2.8$, $n^- = 4.0$) before perihelion. Displayed in Figure 3, the suggested light curve is compared with the naked-eye limiting magnitude in both broad daylight and twilight. The twilight curve is constructed for the most favorable case of the comet and the Sun sharing the same azimuth, i.e., when the comet’s solar elongation equals the difference between the elevations of the comet and the Sun.

⁸ Given that the full moon occurred on Aug 22.5 and Sept 20.9 Chinese time, a scenario that is perfectly compatible with the published record is rather heretic: if Ho’s dates were off (late) by eight days, the first sighting would have been on Aug 26, about four days after the full moon, when the observing conditions greatly improved relative the previous days (as Table 8 shows a month later) and the comet would have disappeared on Sept 21, just hours after the next full moon. Although Ho (1962) provides no information on his methods of conversion of the Chinese calendar to the Julian/Gregorian calendar, we are certain that, barring an inexplicable blunder, the chance of a converted date in the 12th century being off by eight days is nil.

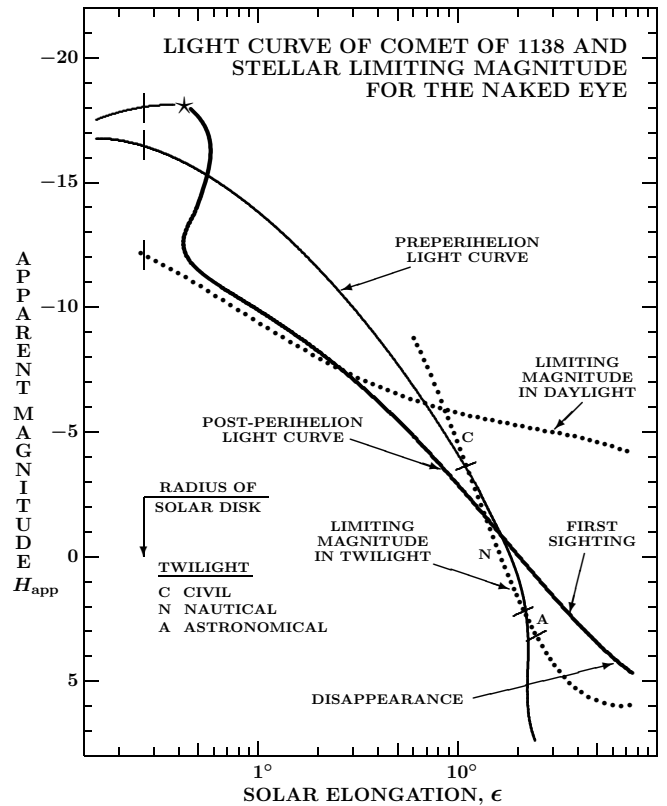


Figure 3. The proposed light curve for the Chinese comet of 1138, plotted as a function of solar elongation. The thin line refers to the preperihelion branch, the thick line to the post-perihelion branch. Perihelion is marked by a star. The points of first sighting on September 3 and the disappearance on September 29 are also indicated. The extent of the solar disk is depicted by short vertical lines. Just before perihelion the comet was passing almost centrally across the Sun. The comet’s light curve is compared with the limiting magnitude of a stellar object for the unaided eye according to Schaefer’s (1993, 1998) algorithm. One limiting-magnitude curve applies to the conditions in broad daylight, the other under twilight’s most favorable conditions when the comet and the Sun have the same azimuth (the solar elongation equaling the difference between the elevations of the comet and the Sun). Boundaries between astronomical, nautical, and civil twilight are shown. No moonlight effects are plotted.

The plot of the light curve in the figure looks rather bizarre, in part because the comet stayed extremely close to the Sun after perihelion for so long. While 12 hours before perihelion the comet was $3^\circ.5$ from the Sun, the separation was less than 1° 12 hours after perihelion! At solar elongations greater than 20° the comet is predicted to have been significantly fainter before perihelion and to have attained apparent magnitude 6 only when 22° from the Sun. It thus must have been entirely out of reach of naked-eye detection. At solar elongations smaller than 15° , the comet is predicted to have been brighter before perihelion and at elongations smaller than 6° it should have been brighter than the naked-eye limiting magnitude. At that time the comet had just a little over 24 hours to get to perihelion. In about six or so hours after perihelion the comet’s brightness dropped to a level close to the limit and stayed near or below that level for at least two weeks, until the comet was some 20° from the Sun. It took only two more weeks (with the Moon

above the horizon in the meantime) before the comet was discovered.

4.4. Tail of the Comet of 1138

Although the historical record quoted by Ho (1962) referred to the comet as a *broom star* — a term used for objects with a tail — no information was provided on the tail’s length. This should not be surprising if the observed tail was unimpressive. An independent investigation of the tails of Kreutz sungrazers (Sekanina, in preparation) shows that some five weeks after perihelion the tails of the 1882 comet and Ikeya-Seki were dominated by microscopic dust subjected to solar radiation accelerations not exceeding 0.6 the solar gravitational acceleration. On September 3 the tail of the 1138 comet should on this condition have been less than 8° long. Theoretically, the length could have grown up to nearly 12° by September 29, but the data on other sungrazers suggest that two months after perihelion only a small fraction of the tail’s computed length could be seen with the naked eye. Because of the geometry, the tail pointed away from the earth. Its end on September 3 is calculated to have been at a geocentric distance of 2.5 AU and it must have been rather faint. The unfavorable geometry (next to moonlight) also explains the short visibility period of the comet.

Kreutz sungrazers become spectacular objects over short periods of time thanks to their early post-perihelion tails (from several days to two weeks after perihelion for comet Ikeya-Seki, for example). The tails are sometimes 10 to 100 times brighter than the head. To become a spectacle, the sungrazer does not have to be a giant, but needs to arrive at the “right” time of the year. The 1138 comet could serve as an example of a sungrazer that arrived at the “wrong” time of the year. Its path in the sky appears to have stayed within one degree of the Sun in the first 12 hours after perihelion, when its predicted light curve in Figure 3 is shaped like a “spiral to obscurity,” losing 8 magnitudes. If the comet had arrived seven weeks later, it could have been comparable in brightness to the Great September Comet of 1882, if 80 days later, it could have been more prominent than Ikeya-Seki. And if it arrived six months earlier or later, it could successfully compete with the appearance of the Great Comet of 1106.

On the other hand, the record of the 1138 comet in historical sources and our sungrazer diagnosis suggest that intrinsically bright Kreutz sungrazers reaching perihelion in early August were not necessarily missed completely — when undetected in broad daylight — by pre-telescopic northern-hemisphere observers, notwithstanding the numerous instances of claim to the contrary in the literature. However, like the comet of 1138, they were likely to have appeared to the naked eye as unimpressive *broom stars* in the morning sky and followed for a few weeks. We suspect that the same argument applies to other bright Kreutz sungrazers that reach perihelion between late May and late July.

5. PERIHELION ASYMMETRY OF PRODUCTION CURVE AND NONGRAVITATIONAL PERTURBATIONS OF A COMET’S ORBITAL MOTION

The outgassing-driven nongravitational perturbations of the sungrazers’ orbital motions, explored in Sec-

tion 3, and the apparent asymmetry of their light curves, examined in Section 4, are of critical importance to our further investigation of the Kreutz system, because there appears to be a degree of correlation between the two parametric functions. This issue was brought to the forefront of attention following the 1986 return of 1P/Halley, as Rickman (1986) and Rickman et al. (1987) argued that the comet’s water production curve showed a strong asymmetry with respect to perihelion, implying that the contributions from the radial component of the sublimation-driven nongravitational force (parameter A_1) integrated over the revolution about the Sun did not cancel out, basically a variation of Bessel’s (1836) concept. In line with this argument, Festou et al. (1990) and Rickman et al. (1992) proposed a hypothesis according to which the water-production asymmetry essentially determines the magnitude of the nongravitational perturbations impacting the orbital period, relegating effects of sublimation lag, expressed by the transverse component (parameter A_2), to the status of a minor factor. While it is inadmissible to use the production-rate asymmetry for determining a magnitude of the outgassing effect on the orbital period (Sekanina 1992, 1993), the two quantities are statistically correlated. And even though Festou et al.’s dataset consisted exclusively of short-period comets, the correlation appears to be valid generally.

In relation to the Kreutz system, this result implies that, as a matter of rule, the orbital motions of the sungrazers that are brighter before perihelion should be slightly accelerated, whereas the motions of the sungrazers brighter after perihelion should be decelerated. This dependence is further correlated with tidal fragmentation near perihelion, as profusely fragmenting sungrazers have a tendency after perihelion to fade less steeply than those subjected to insignificant or no disruption (cf. Paper 2).

It is unfortunate that the symmetric sublimation law still is a universal tool in Marsden et al.’s (1973) orbit-determination software package available to numerous users at present, almost 50 years after it was experimentally incorporated into the nongravitational model that at the time was still in the process of continuing refinement. While it is possible to vary the law’s parameters (such as its steepness, for example), it is not possible to use different functional relations before and after perihelion. Similarly, the law’s peak cannot be moved away from perihelion. There is a version of the Style II formalism with an asymmetric sublimation law in existence, conceived (Sekanina 1988) and implemented (Yeomans & Chodas 1989) to accommodate the nongravitational motions of the short-period comets whose gas production (and activity in general) peaks either profoundly before perihelion (such as 2P/Encke in the early times, 3D/Biela) or after perihelion (such as 1P/Halley, 6P/d’Arrest). However, this type of asymmetric law is not appropriate for application to the sungrazers, whose activity peaks always very near perihelion but the preperihelion and post-perihelion slopes of production curves may be widely uneven. To incorporate a broad range of nongravitational laws in the orbital code should be straightforward, yet no such software package is widely available to our knowledge.

In the broader context, we emphasize the urgent need for solving the long-overdue problem with the sublima-

tion law in orbit-determination software. A wide range of options must be available to the user, in line with the recognized enormous behavior diversity of comets, increasingly perceived in their motions thanks to the steadily improving quality of astrometric observations. In the current versions of orbital software the selection of sublimation laws is mostly limited to the choice of the standard function's constants. By further postponing a radical solution to this problem, the cometary community runs the risk that continuing chronic difficulties will prevent orbital investigations from keeping up with the rapid progress in cometary physics, with which they are increasingly intertwined.

6. LONG-TERM ORBIT INTEGRATION INTO THE PAST: A FEASIBILITY STUDY

To the extent that the Chinese comet of 1106 indeed is the parent body of the Great September Comet of 1882 and comet Ikeya-Seki, the problem of the missing second major Kreutz sungrazer in the early 12th century has been settled. Under these circumstances, the Great Comet of 1106 is perceived, almost by default, as the previous appearance of the Great March Comet of 1843 and a precursor of countless smaller fragments of Population I.

6.1. The Great Comet of 1106

The tail of the comet of 1106 is discussed elsewhere (Sekanina, in preparation); here we display in Figure 4 this spectacular comet's predicted light curve, as a function of solar elongation, to be compared with the predicted light curve of the 1138 comet in Figure 3. In line with Paper 2, we are adopting for the comet of 1106 a set of preperihelion parameters $H_0^- = 2.9$, $n^- = 4.0$ and post-perihelion parameters $H_0^+ = 4.0$ and $n^+ = 4.2$. The assumed preperihelion parameters of the comets of 1106 and 1138 are nearly the same, but after perihelion the 1106 comet is intrinsically four magnitudes *fainter* at 1 AU from the Sun. Although its light curve is steeper, it does not surpass the light curve for the 1138 comet even at that comet's perihelion distance of 0.008 AU.⁹ Yet, the 1106 sungrazer was a spectacle after perihelion, while the performance of the 1138 comet was lackluster.

The perihelion time of the 1106 comet is a point of contention. Hasegawa & Nakano (2001) provide nominally January 26, but there are two caveats: one is the large error, ± 5 days, that the authors put on their value; the other is a report of the comet observed on February 2 only one *cubit* (about 1°) from the Sun in broad daylight (e.g., Kronk 1999). This condition requires the comet to have been no more than several hours past perihelion. On the curve in Figure 4 we accordingly mark the first sighting of the comet for two perihelion times. The observing circumstances long before perihelion appear to have been very favorable, but the comet was then at high southern declinations. As seen from Figures 3 and 4, the 1106 and 1138 comets were both likely to have been several magnitudes brighter than the limit for naked-eye detection in broad daylight just days before perihelion,

⁹ The peak of the 1106 comet's light curve in Figure 4 exceeds the peak of the 1138 comet's light curve in Figure 3 only because the perihelion distance of the former was about two thirds the perihelion distance of the latter.

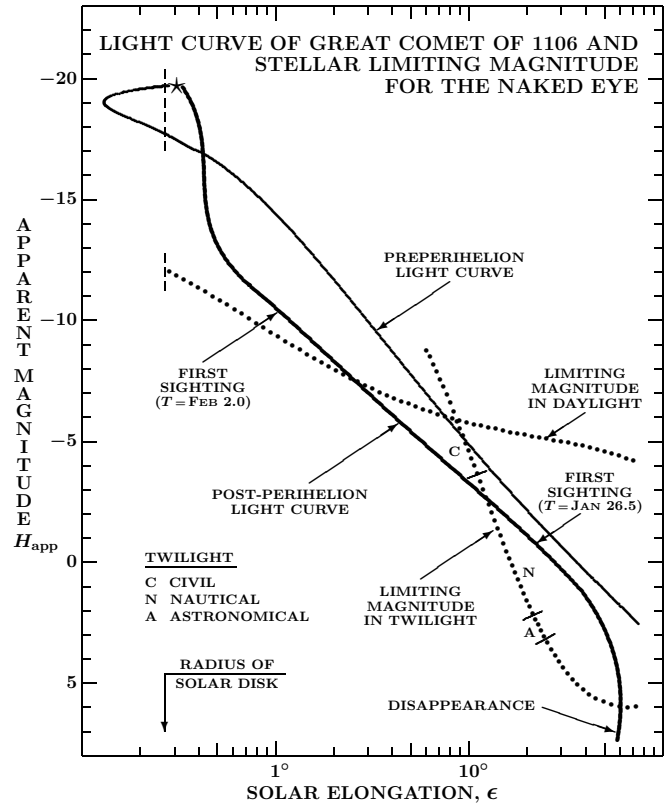


Figure 4. The proposed light curve for the Great Comet of 1106 plotted as a function of solar elongation. The point of first sighting is plotted for two perihelion times, January 26.5 TT and February 2.0 TT. It was argued in Paper 2 that under moderate or better observing conditions historical sungrazers often did not disappear until the head was near magnitude 7, because it was the tail, a few magnitudes brighter, that was last seen. For further comments on the plotted curves, see caption to Figure 3.

yet neither was detected. Except for the early 1106 daylight sighting, the observing periods of the two comets were rather similar, supporting the notion that the 1138 comet was the missing sungrazer.

6.2. Progenitor's Lobe I and Its Main Surviving Mass As the Great March Comet of 1843

The issues that have remained untouched as yet have been those of the early evolution of the Kreutz system. In the contact-binary model (Paper 1), a daytime swarm of brilliant comets in late 363 recorded by Ammianus Marcellinus, a Roman historian, was proposed to be the first perihelion appearance of the Kreutz sungrazers. As separate bodies the sungrazers were less than 500 years old, having originated as a product of fragmentation of the massive progenitor in the general proximity of aphelion near the beginning of the Christian Era.

The primary event was proposed to have been a break-up of the contact-binary progenitor into essentially two lobes — the early precursors of the main populations, I and II — depicted schematically in Figure 5. As already pointed out, the 1843 and 1882 sungrazers were deemed the largest surviving masses of Lobe I and Lobe II, respectively. In line with this scenario, we undertook orbital computations to test the feasibility of the two fundamental steps in the proposed early evolutionary path

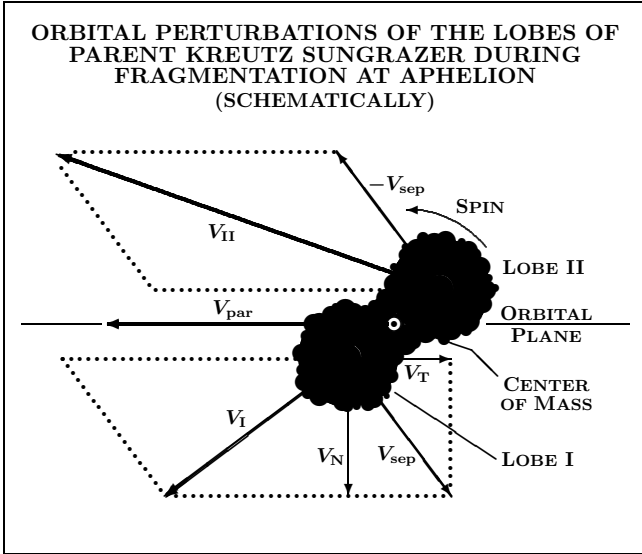


Figure 5. Schematic representation, at the time of breakup, of the Kreutz system’s parent (progenitor) nucleus, modeled as a rotating contact binary in Paper 1, consisting of Lobe I, Lobe II, and the connecting neck. The view is from the direction of the Sun and the position of the original orbital plane is defined by the parent’s pre-breakup orbital velocity vector \mathbf{V}_{par} . The dot in the middle of the neck is the center of mass of the parent, coinciding with the projected spin axis, which at aphelion is assumed to point at the Sun. As a result of the breakup, the lobes are subjected to orbital perturbations. At the time of breakup the comet rotates counterclockwise, so that Lobe I is released to the lower right, moving relative to the center of mass in the direction of the separation velocity vector \mathbf{V}_{sep} , while Lobe II is released to the upper left, moving in the direction of the separation velocity vector $-\mathbf{V}_{\text{sep}}$. The separation velocity consists of its transverse, \mathbf{V}_{T} , and normal, \mathbf{V}_{N} , components, the radial one is assumed to be $\mathbf{V}_{\text{R}} = 0$. Summed up with the parent’s pre-breakup orbital-velocity vector, the separation velocities insert Lobe I into a new orbit defined by the velocity vector \mathbf{V}_{I} and Lobe II into an orbit defined by the velocity vector \mathbf{V}_{II} . The Great March Comet of 1843 is the largest surviving mass of Lobe I, the Great September Comet of 1882 is the largest surviving mass of Lobe II. For clarity, the orbital and separation velocities are not drawn to scale; in the scenario in Paper 1 the ratio $|\mathbf{V}_{\text{sep}}|/|\mathbf{V}_{\text{par}}| = 0.13$.

of the Kreutz system: (i) Could the daylight comets of AD 363 be orbitally linked with the comets of 1106 and 1843 on the one hand and with the comets of 1138 and 1882 on the other hand; and (ii) could Aristotle’s comet of 372 BC be the fragmenting progenitor?

In Section 3 we examined the motions of two observed sungrazer fragments, the products of a presumed tidal breakup of their parent at or near perihelion. Their orbital periods differed dramatically on account of two effects. One of them was triggered by the differential outgassing-driven nongravitational acceleration and accounted for by integration of the continuous contributions from outgassing along the orbit. Long-term effects in the orbital period of this *sublimation scenario* are handled by nongravitational orbital solutions.

Major changes in the orbital period could also be generated as a corollary of tidal fragmentation in close proximity of perihelion. When no momentum exchange is involved, the nascent fragments have the same orbital velocity as the parent, but their centers of mass are located at slightly different heliocentric distances, causing the fragments to end up in orbits with different semima-

ior axes and periods. This is a *fragmentation scenario* whose long-term effects in the orbital period could only be handled by modeling the main features of the fragmentation events, with help of gravitational and/or nongravitational orbital solutions.

In the following we maintain that the evolution of the Kreutz system has been governed by combined effects articulated by the sublimation scenario on the one hand and by the fragmentation scenario on the other hand. While the two categories of effects mix at some unknown variable ratio to scatter sungrazers and their fragments around, we focus below on finding out whether either category can explain — in the entirety or to an extent — the observed properties of the Kreutz system on its own, obviously a more difficult task to accomplish. We have employed the same orbit-determination package of software as in Section 3, fully accounting for both the perturbations by the planets, Pluto, and the three most massive asteroids, as well as for the relativistic and nongravitational effects, using the Style II formalism by Marsden et al. (1973).

Numerical experimentation used in the extensive investigation of comet Ikeya-Seki in Section 3 showed two perplexing features: (i) considerable influence and total unpredictability of the indirect planetary perturbations, which implied the absence of any uniformity or pattern in the sequence of perihelion times; and (ii) problems related to the sublimation law symmetric relative to perihelion, the issue that already was addressed in Section 5. In the absence of an appropriate law, the asymmetry was matched imperfectly by introducing the transverse component of the nongravitational acceleration via the parameter A_2 .

Turning first to the *sublimation scenario*, we attempted to link, in a single orbital run, three consecutive perihelion returns of Lobe I, ending chronologically with the Great March Comet of 1843. The starting set of elements for integration back in time was this comet’s *gravitational* orbit referred to as Solution II in Sekanina & Chodas (2008). It already was optimized to satisfy the 1106 comet’s perihelion time of January 26, proposed by Hasegawa & Nakano (2001), yet it provided an essentially equally good fit to the re-reduced 1843 astrometric observations as the nominal least-squares Solution I. When integrated back to the 4th century, Solution II provided a perihelion time on 392 September 19. The difference of about 29 years needed to fit the adopted perihelion time of 363 November 15 suggested that the comet had been accelerated over the period of nearly 15 centuries (363–1843).

To investigate the magnitude of the acceleration, we incorporated the nongravitational terms into the equations of motion and searched, by trial and error, for the optimum value of the parameter A_2 , while simultaneously adjusting slightly the eccentricity (by about 30 percent of the difference between Solutions I and II in the paper by Sekanina & Chodas 2008). The adopted radial nongravitational parameter A_1 of 10^{-10} AU day $^{-2}$ represents a reasonable value for the nucleus estimated at some 50 km in diameter but, as noted in Section 5, its value has nearly no effect on the results because of the symmetric nongravitational law that the method uses. Very similar orbital solutions could thus be derived with other values of A_1 . The successful linkage of the three consecutive

Table 9

Sublimation Scenario Based Nongravitational Solution for Lobe I Returns of 1843, 1106, and 363 (Equinox J2000)

Orbital element	Perihelion: 1843	Perihelion: 1106	Perihelion: 363
Osculation epoch (TT)	1843 Mar 21.0	1106 Feb 26.0	363 Dec 24.0
Perihelion time (TT)	1843 Feb 27.91423	1106 Jan 26.5	363 Nov 15.2
Argument of perihelion	82°.7555	84°.6889	82°.4109
Longitude of ascending node	3°.6946	5°.8213	3°.0253
Orbit inclination	144°.3839	144°.5358	144°.2040
Perihelion distance (AU)	0.005 460 38	0.005 342 23	0.005 168 17
Orbit eccentricity	0.999 931 65	0.999 935 17	0.999 941 15
Reciprocal semimajor axis (AU ⁻¹)	+0.012 518 04	+0.012 135 26	+0.011 387 73
Orbital period (yr)	714.00	748.04	822.89
Nongravitational parameters (10 ⁻⁸ AU day ⁻²)	A ₁ = +0.01	A ₂ = -0.003 872	A ₃ = 0

returns of Lobe I, presented in Table 9, is manifested by the parametric value of A_2 , which was optimized by first re-fitting the perihelion time in 1106 and then iterating the relationship between the eccentricity and the parameter A_2 until the *previous* perihelion time proposed in Paper 1, 363 Nov 15, was matched. This value of A_2 , shown in Table 9, is smaller than A_2 for any long-period comet in the catalogue by Marsden & Williams (2008). A successful linkage of the perihelion returns in 1843, 1106, and 363 within the framework of the *sublimation scenario* alone is thus shown to be feasible. The parameter A_3 of the normal component of the nongravitational acceleration was assumed to be zero, because this component could not affect the perihelion time.

The linkage of the three consecutive perihelion returns implies that the orbital effect of fragmentation on the Great March Comet of 1843 was insignificant enough that ignoring it did not prevent the formulation of a straightforward nongravitational solution, which over a period of 15 centuries provides supporting evidence for the evolutionary model proposed in Paper 1.

We next turned to the *fragmentation scenario* for Lobe I. The modus operandi was predicated on the fact that one corollary of a breakup is the instantaneous redistribution of a single mass into fragments, accompanied by repositioning of the original center of mass into the centers of mass of the fragments. The small value of A_2 in Table 9 encouraged us to neglect the nongravitational effect altogether. Accordingly, we started from the same gravitational Solution II for the 1843 sungrazer (Sekanina & Chodas 2008). As in the sublimation scenario, we ran the orbit back to 1106 to the point of birth of the 1843 comet, which became the dominant fragment of the Great Comet of 1106, its parent and itself a fragment of the original Lobe I.

The focus of our interest at this point was the nature of the fragmentation event, specifically the separation between the centers of mass of the parent and the fragment along the radius vector (Figure 2). The time of osculation coincided with the time of fragmentation, t_{frg} , assumed to have taken place at perihelion. when in the ecliptical coordinate system the position vector of the center of mass of the nascent 1843 comet was $\mathbf{U}_{\text{frg}} = (X_{\text{frg}}, Y_{\text{frg}}, Z_{\text{frg}})$. The unknown position vector of the center of mass of the parent comet in the ecliptical coordinate system was $\mathbf{U}_{\text{par}} = (X_{\text{par}}, Y_{\text{par}}, Z_{\text{par}})$.

The orbital-velocity vector of the fragment at time t_{frg} , $\mathbf{V}_{\text{frg}} = (X_{\text{frg}}, Y_{\text{frg}}, Z_{\text{frg}})$, together with the position vector determined the fragment's orbit. From Figure 2, the orbital-velocity vector of the parent at t_{frg} , $\mathbf{V}_{\text{par}} = (X_{\text{par}}, Y_{\text{par}}, Z_{\text{par}})$ equaled the fragment's velocity vector. The difference between the position vectors of the 1106 and 1843 comets at t_{frg} imply the existence of one or more additional fragments, which we comment on briefly later.

At a given heliocentric distance of the point of fragmentation, r_{frg} , the position vector of the parent can be derived from the position vector of the fragment and vice versa. The vectorial difference $\Delta\mathbf{U}_{\text{f}\rightarrow\text{p}} = \mathbf{U}_{\text{par}} - \mathbf{U}_{\text{frg}}$ in 1106 depends according to Equation (17) on the orbital period of the parent comet, P_{par} , between the perihelion passages in 1106 and 363, and on the hypothetical orbital period of the fragment, P_{frg} , between 1106 and its past projected perihelion in 392, established by the computations made for this particular case. The derived periods are $P_{\text{par}} = 742.186$ yr and $P_{\text{frg}} = 713.339$ yr.

In the arguments leading to Equation (17) we concluded that, because of the nature of the tidal disruption, the vector $\Delta\mathbf{U}_{\text{f}\rightarrow\text{p}}(\mathbf{r}_{\text{frg}})$ points essentially either in the direction of the radius vector \mathbf{r}_{frg} (when positive) or in the opposite direction (when negative). We replace $\Delta\mathbf{U}_{\text{f}\rightarrow\text{p}}(\mathbf{r}_{\text{frg}})$ with $\Delta U_{\text{f}\rightarrow\text{p}}(r_{\text{frg}})$ and simplify the formula for its magnitude to

$$\Delta U_{\text{f}\rightarrow\text{p}}(r_{\text{frg}}) = \frac{1}{2} r_{\text{frg}}^2 \left(P_{\text{frg}}^{-\frac{2}{3}} - P_{\text{par}}^{-\frac{2}{3}} \right), \quad (24)$$

where $P_k^{-\frac{2}{3}}$ ($k = \text{frg}, \text{par}$) expressed in years are numerically equal to the reciprocal semimajor axes, $1/a_k$, expressed in AU⁻¹, so that $\Delta U_{\text{f}\rightarrow\text{p}}(r_{\text{frg}})$ is in AU. Conversely, $\Delta U_{\text{f}\rightarrow\text{p}}(r_{\text{frg}})$ determines the relationship between the orbital periods P_{par} and P_{frg} :

$$P_{\text{par}} = P_{\text{frg}} \left(1 - \frac{2\Delta U_{\text{f}\rightarrow\text{p}}(r_{\text{frg}})}{r_{\text{frg}}^2} P_{\text{frg}}^{\frac{2}{3}} \right)^{-\frac{3}{2}}. \quad (25)$$

Since we assumed that the 1106 sungrazer fragmented exactly at perihelion, from Table 9 we insert into (24) $r_{\text{frg}} = q = 0.005 342$ AU, which with the above values for P_{frg} and P_{par} yields

$$\Delta U_{\text{f}\rightarrow\text{p}}(q) = +4.662 \times 10^{-9} \text{ AU} = +0.6974 \text{ km}. \quad (26)$$

Table 10

Fragmentation Scenario Based Gravitational Solution for Lobe I Returns of 1843, 1106, and 363 (Equinox J2000)

Orbital element	Perihelion: 1843	Perihelion: 1106	Perihelion: 363
Osculation epoch (TT)	1843 Mar 21.0	1106 Feb 26.0	363 Dec 24.0
Perihelion time (TT)	1843 Feb 27.91423	1106 Jan 26.5	363 Nov 15.0
Argument of perihelion	82° 7555	84° 6888	82° 4113
Longitude of ascending node	3° 6946	5° 8213	3° 0259
Orbit inclination	144° 3839	144° 5359	144° 2041
Perihelion distance (AU)	0.005 460 38	0.005 342 17	0.005 167 92
Orbit eccentricity	0.999 933 39	0.999 935 17	0.999 941 15
Reciprocal semimajor axis (AU ⁻¹)	+0.012 198 69	+0.012 135 00	+0.011 387 45
Orbital period (yr)	742.22	748.07	822.93
Center-of-mass shift $\Delta U_{p \rightarrow f}(r_{\text{frg}})$ (km)			-0.6981
Fragmentation distance r_{frg}			perihelion

Once $\Delta U_{f \rightarrow p}(r_{\text{frg}})$ is known, we proceed to the computation of the orbital elements of the 1106 comet. In a general case, when the point of fragmentation is at a heliocentric distance r_{frg} , the ecliptical coordinates of the parent's position vector at time t_{frg} are

$$\begin{pmatrix} X_{\text{par}} \\ Y_{\text{par}} \\ Z_{\text{par}} \end{pmatrix} = \begin{pmatrix} X_{\text{frg}} \\ Y_{\text{frg}} \\ Z_{\text{frg}} \end{pmatrix} + \Delta U_{f \rightarrow p}(r_{\text{frg}}) \begin{pmatrix} P_x & Q_x \\ P_y & Q_y \\ P_z & Q_z \end{pmatrix} \times \begin{pmatrix} \cos u_{\text{frg}} \\ \sin u_{\text{frg}} \end{pmatrix}, \quad (27)$$

where P_x, \dots, Q_z are the standard direction cosines and u_{frg} is the true anomaly at fragmentation. In the case of fragmentation at perihelion the transformation formulas get simplified accordingly. Since the indirect planetary perturbations may change slightly the orbit, one may not obtain the prescribed perihelion time of 363 November 15 exactly, and one or more iterations may be necessary. Indeed, the value of $\Delta U_{f \rightarrow p}$ had to be changed from 0.6974 km to 0.6981 km to fit the adopted perihelion time in 363 exactly.

The sets of gravitational orbital elements of Lobe I at the three returns to perihelion between 363 and 1843, based on the fragmentation scenario, are listed in Table 10. Comparison with Table 9 shows that the differences in all the elements between the two categories of orbits are trivial, with the possible exception of the orbital period. An obvious conclusion is that applications of both the sublimation scenario and the fragmentation scenario, either one on its own, satisfy the constraints of the evolutionary model of the Kreutz system over the 15 centuries. Orbit integration prior to the year 363 and its ramifications will be addressed in Section 7.

6.3. Possible Nuclear Sizes of Comets 1106 and 1843 and Population of Minor Kreutz Comets

The shift $\Delta U_{f \rightarrow p}$ between the parent and a fragment is an important quantity that provides information on the fragment's approximate dimensions and their relationship to the parent's dimensions. In general terms, the smaller the shift, the larger the fragment's size. Although no reliable data are available, the nucleus of the 1882 sungrazer was crudely estimated at 50 km in diameter (Sekanina 2002), and the 1843 and 1882 sungrazers are probably of comparable sizes. From this vantage point, a shift in the position of the center of mass by

mere 0.7 km is strong evidence that during the perihelion breakup of the 1106 comet most mass remained concentrated in one fragment — the 1843 sungrazer. Since the shift is sunward — measured from the parent to the fragment — minor fragments were at the antisunward end of the parent, while its sunward half did not fragment at all; in Figure 2 this fits Scenario I.

On certain assumptions about the shape of the parent object, one can provide even some quantitative estimates. Let the parent be approximated by a prolate spheroid of an arbitrary axial ratio, whose long axis pointed at the time of fragmentation toward the Sun, and let the dominant fragment, in this case the 1843 sungrazer, be represented by a truncated prolate spheroid, which extends from one end of the spheroid to a plane normal to the long axis at a certain distance, d , from that end. Assigning the parent's spheroid a unit volume, we measure, in these units, the volume \mathfrak{R} of the truncated spheroid by a dimensionless parameter ζ , which equals the ratio of the distance d to the extent of the long axis:

$$\mathfrak{R}(\zeta) = 3\zeta^2 \left(1 - \frac{2}{3}\zeta\right). \quad (28)$$

The parent's center of mass is given by $\zeta = \frac{1}{2}$, whereas the fragment's center of mass has obviously $\zeta < \frac{1}{2}$. The volume of the truncated spheroid needs to be expressed in terms of $\Delta U_{f \rightarrow p}$. In order to do that, we introduce a dimensionless quantity, ψ , by

$$\Delta U_{f \rightarrow p} = \psi \mathcal{R}, \quad (29)$$

where \mathcal{R} is the radius of the spheroid's long axis. The normalized volume of the truncated spheroid is then

$$\mathfrak{R}(\psi) = 1 - \frac{3}{2}\psi \left(1 - \frac{1}{3}\psi^2\right). \quad (30)$$

Inserting for \mathfrak{R} from (30) into (28), we find the length d of the truncated spheroid by solving for ζ :

$$d = 2\mathcal{R}\zeta = \frac{\mathcal{R}\sqrt{\mathfrak{R}(\psi)}}{\cos\left[\frac{1}{3}\arccos\left(-\sqrt{\mathfrak{R}(\psi)}\right)\right]} \quad (31)$$

Approximating the size of the prolate spheroid for the 1106 comet's nucleus by $\mathcal{R} = 28$ km, we have $\psi = 0.025$, from (30) $\mathfrak{R} = 0.9625$, and from (31) $d = 49.5$ km, or near the estimated nuclear diameter of the 1843 sungrazer.

The remaining part of the spheroid, modeled as a spheroidal cap, is in this case 6.5 km long and has a volume of 3.75 percent of the parent. Its center of mass is 23.5 km from the center of mass of the parent and its calculated orbital period exceeds 20,000 years. This mass is essentially lost to the system and it may never be discovered.

Up to now we only considered tidal breakups taking place exactly at perihelion and separation of fragments from the long end of a spheroidal nucleus. In reality, tidal fragmentation events may have happened (or continued happening) shortly before or after perihelion, in which case the shifts $\Delta U_{f \rightarrow p}(r_{\text{frag}})$ increased in magnitude and the orbital periods of large numbers of fragments were confined to a narrower range, many exceeding the orbital period of the parent by less than a factor of two. In addition, the parent's nucleus was unquestionably an irregular body with variable tensile strength, so that tidal fragmentation proceeded in parts other than one end of its longest dimension as well. Finally, especially minor fragments could have been shed from the body of the parent/main fragment by forces other than tidal; in the extremely hostile environment of the Sun's inner corona such mass shedding should be part of the bulk fragmentation process. As long as the shedding is accompanied by no momentum exchange, the fragments end up essentially in the orbits governed by $\Delta U_{f \rightarrow p}(r_{\text{frag}})$.

In this context we note that the separation times for the individual nuclei of the Great September Comet of 1882, derived from their observed separations by Sekanina & Chodas (2007), averaged 1.8 hours after perihelion, at which time the comet's heliocentric distance was twice the perihelion distance, or $3.3 R_{\odot}$. For the 1843 sungrazer the corresponding fragmentation distance would be $2.3 R_{\odot}$. At such a distance, a large number of Kreutz sungrazers and potential Kreutz sungrazers of Population I could be fitted as fragments of the 1106/1843 comet with moderate ΔU shifts. A shift of about -20 km could explain the concentration (or at least a major contribution to the concentration) of potential Kreutz sungrazers in the middle and the second half of the 17th century, including the candidate comets of 1663, 1666, 1668, 1673, and 1695 on Hasegawa & Nakano's (2001) list. Positive values of ΔU could apply to a number of known Kreutz sungrazers: for example, ~ 3.5 km fits C/1880 C1 and C/1882 K1, the eclipse sungrazer;¹⁰ ~ 11.5 km fits the sungrazers picked up by the coronagraphs on board the Solwind (P78-1) and Solar Maximum Mission satellites; and 12 to 14 km fits the SOHO and STEREO sungrazers from the 1990s through 2020s, whose orbital periods should be close to 900 years. An exception is comet Pereyra (C/1963 R1), which appears to be a fragment of another subcategory of Population I and its evolution is briefly described in Section 8.

6.4. *Orbital Relationship Between the Great September Comet of 1882 and Comet Ikeya-Seki*

Before we examine the sublimation and fragmentation scenarios of the comet of 1138, we return to the problem of the pre-fragmentation orbit of comet Ikeya-Seki and its

¹⁰ However, the 1880 sungrazer may have separated from the 1106 comet at large heliocentric distance; C/1887 B1 very probably separated subsequently from the 1880 comet (Paper 1).

relationship to the orbit of the Great September Comet of 1882. A major point of Marsden's (1967) paper was his virtual proof that on approach to the previous perihelion in the 12th century the two comets were one.

Our surprising conclusion that Ikeya-Seki was previously at perihelion as the Chinese comet of 1138 more than 30 years after the Great Comet of 1106 was not accompanied by the full set of elements of the pre-fragmentation orbit. In the meantime, we were pursuing several avenues in an effort to determine such an orbital set, but were repeatedly encountering a variety of problems. Our ultimate choice was based on an inference from the perturbation theory that a fragmentation event at perihelion, not involving momentum exchange, measurably affects the orbital period (or, equivalently, the semimajor axis or eccentricity) but not the other five elements. Their post-perihelion variations have roots mostly in the nongravitational forces, so that — again with the exception of the eccentricity and equivalent elements — the orbit of the most massive fragment should provide the closest approximation to the orbit of the pre-fragmentation comet. For Ikeya-Seki, the most massive fragment was unequivocally nucleus A.

The same argument suggested that among the fragments of the Great September Comet of 1882 it was its nucleus B (or No.2 in Kreutz's notation) that should provide the best approximation to the comet's pre-fragmentation orbit. The orbit of this nucleus, presented in the Appendix, was our first choice for the purpose of comparison with the orbit of comet Ikeya-Seki, in spite of the fact that it is nonrelativistic.¹¹

Our first concern was the time of the previous perihelion of the comet's nucleus B, for which we obtained 1136 January 23; formal inclusion of the relativistic effect moved the perihelion forward by merely 37 days. As the mean error of the orbital period is shown in the Appendix to amount to ± 2.8 yr, the estimated perihelion time of the 1138 comet remained within 1σ of the predicted time of the 1882 comet's previous return to perihelion. The very fact that the integration of this nucleus' orbital motion offered the "correct" time for the previous return to perihelion of the pre-fragmentation nucleus of the 1882 sungrazer is astonishing and its interpretations range from sheer coincidence to evidence that fragment B was indeed the primary nucleus, orders of magnitude more massive than any other among the five or six major fragments reported.

Of primary interest to us were the sets of orbital elements of the 1882 sungrazer and comet Ikeya-Seki in August 1138. To make it meaningful, we computed the orbit of Ikeya-Seki *without* the relativistic effect to match the same quality of the orbital set available for the 1882 sungrazer. We integrated the orbits of both comets back in time, adjusting in either case the eccentricity to force the previous perihelion on 1138 August 1. In essence, we applied the same test as Marsden (1967) did in his paper: aiming at comparison of the orbits of the 1882 comet's nucleus B and Ikeya-Seki's nucleus A at the time of their presumed separation. The difference was that Marsden

¹¹ The theory of general relativity, including its orbital ramifications, was introduced by A. Einstein in 1915, just about a quarter-century after Kreutz's publication of the definitive orbits for the nuclear fragments of the 1882 sungrazer in the second paper of the series.

Table 11
Relationship Between Nonrelativistic Orbits of the Great September Comet of 1882 and Comet Ikeya-Seki
With Eccentricity Adjusted to Fit Perihelion of the Comet of 1138 (Equinox J2000)

Orbital element	1882 sungrazer		Ikeya-Seki		Difference ^a in Aug 1138 (this paper)	Difference ^a in Mar 1115 (Marsden)	Ratio ^b of 1138/1115 differences
	in 1882	in 1138	in 1965	in 1138			
Osculation epoch (TT)	1882 Oct 2.0	1138 Sept 6.0	1965 Oct 7.0	1138 Sept 6.0
Perihelion time (TT)	1882 Sept 17.72404	1138 Aug 1.0	1965 Oct 21.18368	1138 Aug 1.0
Argument of perihelion	69°.58477	67°.28090	69°.04914	67°.28565	-0°.004 75	+0°.013	0.365
Longitude of ascending node	347°.65640	344°.67570	346°.99465	344°.67703	-0°.001 33	+0°.019	0.070
Orbit inclination	142°.01104	141°.35349	141°.86426	141°.35379	-0°.000 30	+0°.004	0.075
Perihelion distance (AU)	0.007 750 29	0.008 044 92	0.007 785 40	0.008 048 00	-0.000 003 08	+0.000 006 0	0.513
Orbit eccentricity	0.999 907 69	0.999 902 92	0.999 913 58	0.999 909 57
Reciprocal semimajor axis (AU ⁻¹)	+0.011 909 90	+0.012 066 73	+0.011 099 49	+0.011 236 59
Orbital period (yr)	769.37	754.42	855.16	839.55

Notes.

^a Difference in the orbital element between the 1882 sungrazer and Ikeya-Seki.

^b Absolute value of the ratio of the orbital difference between the two comets in 1138 presented in this paper to their difference in 1115 listed in Table X of Marsden (1967).

assumed the separation in September 1115, whereas our target date was some 23 years later. The outcome is presented in Table 11; the elements for an osculation epoch in the start-up years of 1882 and 1965 are, respectively, in columns 2 and 4; the 1138 elements in columns 3 and 5. The degree of similarity between the two comets in the four relevant elements in 1138 is apparent from column 6; the degree of similarity that Marsden (1967) found in 1115 is copied in column 7. Besides the fact that all 1138 differences were of opposite sign than the 1115 differences, their comparison, in terms of an absolute value of the 1138-to-1115 ratio, offers a stunning result: the *orbital elements of the two comets were much more alike in 1138*, the nodal longitude and the inclination by more than one order of magnitude(!), the argument of perihelion by a factor of nearly 3, and the perihelion distance by a factor of about 2. The near-coincidence of the orbits of the two comets in 1138 is equally impressive when measured by the mean errors of Kreutz's elements in the Appendix: the differences in the nodal longitude and inclination are smaller than 0.5σ (!), in the argument of perihelion about 2σ , and in the perihelion distance, the worst case, a little over 3σ . The tiny differences in the nodal longitude and inclination show that orbital planes of the two comets deviated from each other in 1138 less than was the uncertainty of the 1882 comet's orbital-plane determination. The obvious conclusion is that the year 1138 was a much better choice for separating Ikeya-Seki from the 1882 sungrazer than the year 1115, not to mention 1106. This is yet another piece of evidence that contradicts the hypothesis of the 1106 comet being the parent to the 1882/1965 pair.

6.5. *Progenitor's Lobe II and Its Main Surviving Mass As the Great September Comet of 1882*

The resemblance of the orbital elements (except for the period and equivalent quantities) between the 1882 sungrazer and Ikeya-Seki in the year 1138 is so profound that a tight relationship between the two objects cannot be doubted. In the context of the contact-binary model, their parent — and later the 1882 sungrazer — was the largest surviving mass of Lobe II of the Kreutz system's

progenitor (Figure 5). Long-term orbit integration of the motion of Lobe II was carried out in the same manner as that of Lobe I in Sections 6.2 and 6.3, engaging, respectively, the *sublimation* and *fragmentation* scenarios.

To test the feasibility of a single orbital run linking three consecutive returns of Lobe II, we again employed Kreutz's (1891) gravitational (nonrelativistic) orbit of nucleus B (see the Appendix) but used, from now on, orbit-determination software with the relativistic effect built in. As expected, a fairly minor adjustment in the eccentricity was needed to fit the adopted perihelion time of the 1138 comet. The previous perihelion was computed to have occurred on 459 Jan 29, nearly a century later than the expected year 363, implying that Lobe II was subjected to a much higher nongravitational acceleration than Lobe I. The results of the search for a nongravitational solution consistent with the sublimation scenario confirmed the suspicion. As shown in Table 12, the required magnitude of the transverse acceleration was now more than twice the adopted magnitude of the radial acceleration and more than five times the transverse acceleration for the 1843 comet (Table 9). In case of the 1882 sungrazer the effects that we tried to account for by the nongravitational parameter A_2 appear to have been governed by fragmentation rather than by sublimation.

Application of the fragmentation scenario based procedures in the case of Lobe II was much more involved than it had been for Lobe I in Section 6.2. Before we began to investigate Lobe I, we did not know whether it fragmented profusely, modestly, or not at all. On the other hand, unquestionable evidence on fragmentation of Lobe II was offered by the breakup of the 1882 sungrazer and Ikeya-Seki, which had to be accommodated by the contact-binary model. Referring to them as fragments f_1 (the 1882 sungrazer) and f_2 (Ikeya-Seki), respectively, the constraint provided by their orbital periods ($P_{f_1} = 744.084$ yr and $P_{f_2} = 827.172$ yr) was

$$\Delta U_{f_1 \rightarrow f_2}(r_{\text{frg}}) = +4.02 \left(\frac{r_{\text{frg}}}{q} \right)^2 \text{ km} \quad (32)$$

Here ΔU has the meaning of the radial distance be-

Table 12

Sublimation Scenario Based Nongravitational Solution for Lobe II Returns of 1882, 1138, and 363 (Equinox J2000)

Orbital element	Perihelion: 1882	Perihelion: 1138	Perihelion: 363
Osculation epoch (TT)	1882 Oct 2.0	1138 Sept 6.0	363 Dec 24.0
Perihelion time (TT)	1882 Sept 17.72404	1138 Aug 1.0	363 Nov 15.0
Argument of perihelion	69°.5847	67°.2809	64°.9196
Longitude of ascending node	347°.6564	344°.6757	341°.7698
Orbit inclination	142°.0110	141°.3535	140°.3872
Perihelion distance (AU)	0.007 750 24	0.008 045 23	0.008 448 11
Orbit eccentricity	0.999 898 92	0.999 902 92	0.999 906 95
Reciprocal semimajor axis (AU ⁻¹)	+0.013 042 48	+0.012 066 90	+0.011 015 26
Orbital period (yr)	671.37	754.41	864.98
Nongravitational parameters (10 ⁻⁸ AU day ⁻²)	A ₁ = +0.01	A ₂ = -0.020 559	A ₃ = 0

tween the centers of mass of the two fragments. If the 1882 sungrazer and Ikeya-Seki had irregular nuclei some 50 km and 10 km, respectively, in diameter, their centers of mass could hardly be separated by less than ~ 20 km, which means that the fragmentation event of this kind could not have taken place closer to the Sun than ~ 2.2 times the perihelion distance, or about 0.018 AU (or nearly 4 solar radii) from the Sun, at least 2.2 hr before or after perihelion.

The second constraint for Lobe II was provided by the difference between the projected motion of the 1882 sungrazer integrated back in time from its 1138 perihelion to the previous hypothetical perihelion passage, on 459 January 29 — implying an orbital period of $P_{\text{frg}} = 679.491$ yr — and the corrected motion dictated by the expected perihelion of the parent on 363 November 15, implying $P_{\text{par}} = 774.696$ yr. The computations showed that the required shift of the center of mass at the 1138 perihelion equaled

$$\Delta U_{f \rightarrow p}(q) = +5.2499 \text{ km}, \quad (33)$$

an effect that was a factor of 7.5 greater than in the case of Lobe I, shown in (26).

The motion of Lobe II between the returns of 363 and 1138 is determined by the condition (33); the sets of representative gravitational orbital elements in the returns of 1882, 1138, and 363, based on the fragmentation scenario, are listed in Table 13. To accommodate the conditions (32) and (33) during the 1138 perihelion passage, we assumed again that the parent comet, approaching perihelion was a prolate spheroid of an arbitrary axial ratio and an unknown long-axis diameter \mathcal{D} , which was to be determined from the constraint (33). As in the case of Lobe I, we were addressing the problem in terms of dimensionless quantities, in units of \mathcal{D} . We further assumed that the parent split first into two at perihelion, satisfying (33), followed by the separation of the major fragment into the 1882 sungrazer and Ikeya-Seki hours later.

Let us adopt for the 1882 sungrazer a diameter of 50 km and for Ikeya-Seki a diameter of 10 km in the direction of the spheroid's long axis, so that $\mathcal{D} > 60$ km. In Figure 6 we draw the points on the spheroid's axis that describe the fragmentation events. With the Sun to the right, the points refer to the first breakup in the upper panel and to the second breakup in the lower panel. In either

panel A is the sunward end of both the surviving mass of Lobe II and the 1882 sungrazer, O the center of mass of Lobe II, C the center of mass of the 1882/1965 pair's parent, B its antisolar end, and W the boundary between the 1882 sungrazer and Ikeya-Seki inside Lobe II. In addition, in the upper panel, Z is the antisolar end of Lobe II, so that B and Z are the boundaries of the minor fragment that separated at perihelion, and G is its center of mass. In the lower panel, E and F are the centers of mass of, respectively, the 1882 sungrazer and Ikeya-Seki. Since $AZ = 1$ and $AO = OZ = \frac{1}{2}$, the normalized size of the 1882 sungrazer is $\alpha = \overline{AW} = 50/\mathcal{D}$ and the normalized size of Ikeya-Seki $\beta = \overline{WB} = 10/\mathcal{D}$. The size of their parent is of course $\gamma = \overline{AB} = \alpha + \beta = 60/\mathcal{D}$ and the size of the minor fragment separating at perihelion is $\epsilon = \overline{BZ} = 1 - \gamma = (\mathcal{D} - 60)/\mathcal{D}$. We further denote the dimensionless distances from A of the centers of mass of, respectively, the 1882 sungrazer, Ikeya-Seki, their parent, and the minor fragment by $\alpha' = \overline{AE}$, $\beta' = \overline{WF}$, $\gamma' = \overline{AC}$, and $\epsilon' = \overline{GZ}$. We count the distances positive in the direction away from the Sun, and vice versa.

Given that the normalized volume of a truncated spheroid, \mathfrak{R} , varies with the distance from the apex as indicated by (28), we have for the parent of the 1882/1965 pair, separating from the minor fragment in the course of the perihelion event, $\mathfrak{R}(\gamma) = 3\gamma^2(1 - \frac{2}{3}\gamma)$, as is schematically shown in the top panel of Figure 6. Following (31),

$$\gamma = \frac{60}{\mathcal{D}} = \frac{\sqrt{\mathfrak{R}(\gamma)}}{2 \cos \left\{ \frac{1}{3} \arccos \left[-\sqrt{\mathfrak{R}(\gamma)} \right] \right\}}. \quad (34)$$

Since the coordinate of the center of mass of the truncated spheroid has to halve its volume, we equate

$$\mathfrak{R}(\gamma') = \frac{1}{2} \mathfrak{R}(\gamma). \quad (35)$$

On the other hand, from (33) and Figure 6 it follows that

$$\gamma' = \frac{1}{2} - \frac{\Delta U_{f \rightarrow p}(q)}{\mathcal{D}} = \frac{1}{2} - \frac{5.244}{\mathcal{D}}. \quad (36)$$

The diameter \mathcal{D} in (34) and (36) is given in km. Combining (34) through (36), we find that the ratio

$$K = \frac{\frac{1}{2} - \gamma'}{\gamma} = 0.0875, \quad (37)$$

Table 13

Fragmentation Scenario Based Gravitational Solution for Lobe II Returns of 1882, 1138, and 363 (Equinox J2000)

Orbital element	Perihelion: 1882	Perihelion: 1138	Perihelion: 363
Osculation epoch (TT)	1882 Oct 2.0	1138 Sept 6.0	363 Dec 24.0
Perihelion time (TT)	1882 Sept 17.72404	1138 Aug 1.0	363 Nov 15.0
Argument of perihelion	69°.5848	67°.2809	64°.9195
Longitude of ascending node	347°.6564	344°.6757	341°.7697
Orbit inclination	142°.0110	141°.3535	140°.3871
Perihelion distance (AU)	0.007 750 29	0.008 044 92	0.008 446 37
Orbit eccentricity	0.999 907 69	0.999 902 92	0.999 906 96
Reciprocal semimajor axis (AU ⁻¹)	+0.011 909 90	+0.012 066 73	+0.011 015 12
Orbital period (yr)	769.37	754.42	865.00
Center-of-mass shift $\Delta U_{p \rightarrow f}(r_{\text{frg}})$ (km)		-5.2499	
Fragmentation distance r_{frg}		perihelion	

which allows one to determine the normalized volume of the 1882/1965 parent shaped as a truncated spheroid, $\mathfrak{R}(\gamma) = \mathfrak{R}$, given that

$$K = \mathfrak{R}^{-\frac{1}{2}} \cos \left[\frac{1}{3} \arccos(-\sqrt{\mathfrak{R}}) \right] \times \left\{ 1 - \frac{\sqrt{2\mathfrak{R}}}{2 \cos \left[\frac{1}{3} \arccos \left(-\frac{1}{2} \sqrt{2\mathfrak{R}} \right) \right]} \right\}. \quad (38)$$

The normalized length γ follows from (34) and so does \mathcal{D} . Numerically,

$$\begin{aligned} \mathfrak{R}(\gamma) &= 0.81142, \\ \gamma &= 0.72225, \\ \gamma' &= 0.43680, \\ \mathcal{D} &= 83.07 \text{ km}. \end{aligned} \quad (39)$$

In addition, the diameter of the minor fragment separating at perihelion is determined to equal about 23 km and the distance of its center of mass from the center of Lobe II 25.8 km. Following the separation, this fragment ended up in an orbit with a period of about 1800 yr.

The major fragment, which was to split into the 1882 comet and Ikeya-Seki, continued to orbit the Sun as a single body, until (32) was satisfied. To determine the distance, Ψ , between the centers of mass of the 1882 sungrazer and Ikeya-Seki, the following conditions apply:

$$\begin{aligned} \mathfrak{R}(\alpha') &= \frac{1}{2} \mathfrak{R}(\alpha), \\ \mathfrak{R}(\beta' + \alpha) &= \frac{1}{2} [\mathfrak{R}(\alpha) + \mathfrak{R}(\gamma)], \\ \Psi &= [(\beta' + \alpha) - \alpha'] \mathcal{D}. \end{aligned} \quad (40)$$

Since $\alpha = 0.60190$, we obtain $\mathfrak{R}(\alpha) = 0.65073$, from the first equation of (40) $\alpha' = 0.38135$, from the second equation $\beta' = 0.05756$, and from the third equation $\Psi = 23.1$ km. Inserted into (32), the required fragmentation distance is $r_{\text{frg}} = 2.40 q = 0.0193 \text{ AU} = 4.15 R_{\odot}$.

The reader may notice that the procedure is approximate, one reason being that the condition (32), which applies to the center of mass of the 1882 sungrazer, was assigned instead to the center of mass of the 1882/1965 pair. Since the distance between them amounted to $(\gamma' - \alpha')\mathcal{D} = 4.61$ km, the center-of-mass shift of the parent at perihelion was only $5.25 - 4.61 = 0.64$ km, so that

$K = 0.0107$, $\mathfrak{R}(\gamma) = 0.9712$, and $\gamma = 0.89853$. The parent's size then equaled merely ~ 67 km. These improved results (and further iterations) have of course no effect on our simulation of the motion of Lobe II before 1138.

7. KREUTZ SUNGRAZERS AT PERIHELION IN AD 363, APHELION BREAKUP OF CONTACT-BINARY PARENT, AND ITS PRE-FRAGMENTATION ORBIT

In the context of the contact-binary model, it was postulated that the largest surviving mass of Lobe I appeared most recently as the Great March Comet of 1843

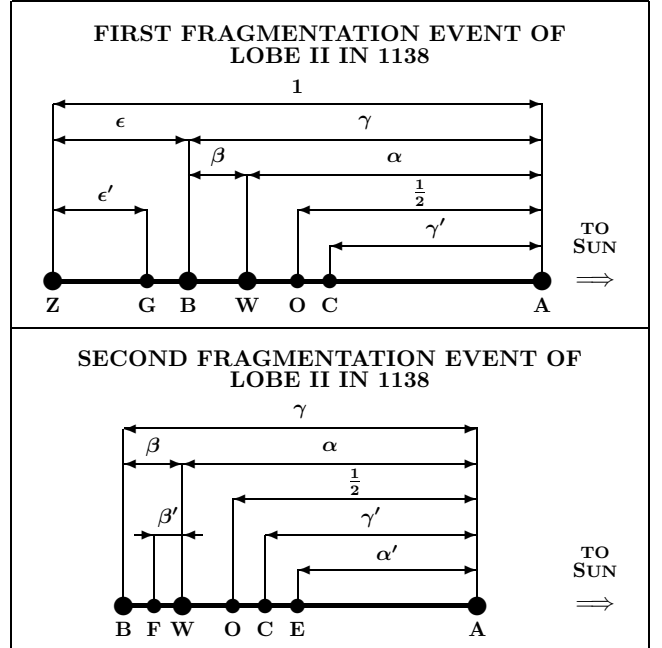


Figure 6. Relative sizes and center-of-mass positions of the Lobe II parent and its fragments in the two fragmentation events in 1138. In the first event (top), the long axis of the prolate-spheroidal parent is unity, the parent of the 1882 sungrazer (α) and Ikeya-Seki (β) is γ (being truncated at B, the size of the minor fragment is ϵ). The position of the parent's center of mass is at O, the center of mass of the parent of the 1882 sungrazer and Ikeya-Seki is at G, and the center of mass of the minor fragment is at C. In the second fragmentation event, Ikeya-Seki separated from the 1882 comet (bottom); their centers of mass are at F and E, respectively.

Table 14

Predicted Fragmentation Scenario Based Gravitational Solutions for Lobes I and II in 363 and (Extrapolated) –371 (Equinox J2000)

Orbital element	L o b e I		L o b e II	
	Perihelion: AD 363	Perihelion: 372 BC	Perihelion: AD 363	Perihelion: 372 BC
Osculation epoch (TT)	363 Dec 24.0	–371 Jan 11.0	363 Dec 24.0	–371 Jan 11.0
Perihelion time (TT)	363 Nov 15.0	–371 Jan 1.0	363 Nov 15.0	–371 Jan 1.0
Argument of perihelion	82°.4113	77°.3356	64°.9195	61°.9165
Longitude of ascending node	3°.0259	356°.7567	341°.7697	337°.8229
Orbit inclination	144°.2041	143°.4681	140°.3871	139°.0175
Perihelion distance (AU)	0.005 167 91	0.005 222 90	0.008 446 34	0.008 721 03
Orbit eccentricity	0.999 937 93	0.999 938 78	0.999 898 56	0.999 897 92
Reciprocal semimajor axis (AU ^{–1})	+0.012 011 36	+0.011 722 03	+0.012 009 74	+0.011 704 80
Orbital period (yr)	759.65	787.94	759.80	789.68
Center-of-mass shift $\Delta U_{p \rightarrow f}(r_{\text{frg}})$ (km)		+1.2462		+5.3071
Fragmentation distance r_{frg}		perihelion		perihelion

and, before, as the Great Comet of 1106. Similarly, the largest surviving mass of Lobe II appeared most recently as the Great September Comet of 1882 and, before, as the Chinese comet of 1138. The arrival of Lobe II lagged behind Lobe I by $39\frac{1}{2}$ yr in the 19th century and by $32\frac{1}{2}$ yr in the 12th century.

7.1. Kreutz Sungrazers at Perihelion in AD 363

The spectacle of brilliant daylight comets in AD 363, recorded for posterity by Ammianus Marcellinus, a Roman historian,¹² was simulated in this feasibility study as the first perihelion appearance of the Kreutz system after the progenitor’s fragmentation at large heliocentric distance. It differed from the subsequent perihelion returns (in the 12th and 19th centuries) in that *both* Lobe I and Lobe II contributed virtually simultaneously to the event. We have shown that the perihelion returns 1843–1106–363 and 1882–1138–363 could both be linked in the framework of either the sublimation scenario or the fragmentation scenario, even though the high value of the critical nongravitational parameter for Lobe II made the veracity of the sublimation scenario suspect.

Since fragmentation events at large heliocentric distance are known to have a fairly minor effect on the perihelion time, we used the fragmentation-scenario tools to derive the center-of-mass shifts ΔU in an effort to determine the preliminary sets of orbital elements for Lobe I and Lobe II in the period of time between 363 November 15 and the previous perihelion on –371 January 1. The results are presented in Table 14. The two orbits for the progenitor in 372 BC are of course artificial; the ultimate orbit is going to be the product of simulation of the process of near-aphelion fragmentation (Sections 7.2 and 7.3).

Comparison of Tables 10 and 14 for Lobe I and Tables 13 and 14 for Lobe II reveals a major difference between the 12th century returns on the one hand and AD 363 on the other hand: the center of mass of the *major* fragment was located sunward of the parent object in 1106 and 1138 ($\Delta U_{p \rightarrow f} < 0$; Scenario I in Figure 2), but antisunward in AD 363 ($\Delta U_{p \rightarrow f} > 0$; Scenario II in

Figure 2). This difference has an important ramification. Scenario I implies that a typical *minor* fragment, or most minor fragments, should have the center(s) of mass on the antisunward side of the parent’s center of mass, should end up in highly elongated orbits, with the periods much longer than 700–800 yr, and should not return to perihelion until some time in the distant future. By contrast, Scenario II implies that minor fragments have typically the centers of mass on the sunward side of the parent’s center of mass, ending up in orbits with the periods shorter, and potentially much shorter, than 700–800 yr. Such fragments might have become sungrazers in their own right during the centuries following the year 363, starting as early as the 6th century.

To inspect this issue quantitatively, we employ a relationship analogous to (25), expressing the orbital period of a fragment, P_{frg} , as a function of the orbital period of the parent, P_{par} , rather than vice versa:

$$P_{\text{frg}} = P_{\text{par}} \left(1 - \frac{2\Delta U_{p \rightarrow f}(r_{\text{frg}})}{r_{\text{frg}}^2} P_{\text{par}}^{\frac{2}{3}} \right)^{-\frac{3}{2}}. \quad (41)$$

Suppose, for the sake of argument, that Lobes I and II were in AD 363 nearly 100 km across each and that a reasonable upper limit on the center-of-mass shift of a fragment was about 45 km. Table 15 presents the orbital periods that the fragments acquire as a function of (i) the heliocentric distance at fragmentation (q being again the perihelion distance) and (ii) the center-of-mass shift relative to the parent comet in AD 363 (see Table 14). It is astonishing to see that in an extreme case the orbital period could be as short as one-fifth the parent’s orbital period (~ 760 yr) for Lobe I and less than one-half of it for Lobe II.

In a second experiment, we picked up four of the potential Kreutz sungrazers from Hasegawa & Nakano’s (2001) list in the 7th through 11th century and computed the center-of-mass shifts that would be required if the comets were fragments of Lobe I or Lobe II released at the 363 perihelion. It is seen that their orbits could readily be accommodated this way, with the exception of the comet of 607, which could not be a fragment of Lobe II.

¹² See Paper 1 for details and useful references on this subject.

From (41) it is obvious that the relation between the orbital periods of the parent and a fragment is governed by the ratio of $\Delta U/r_{\text{frg}}^2$. The effect drops very rapidly with increasing distance from the Sun but also with decreasing size of the object and its orbit. In practice it has no meaningful application to fragmenting comets other than sungrazers.

7.2. Line of Intersection of Lobes' Orbital Planes and Positions of Lobes at Fragmentation Time

In order to successfully simulate the separation of the two lobes from the contact-binary progenitor near aphelion, three conditions have to be satisfied in the barycentric system: (i) the point of separation must be located on the line of intersection of the lobes' orbital planes; (ii) the lobes must be at the same barycentric distance; and (iii) they must reach the point simultaneously. Given that the tabulated orbits are available at an osculation epoch near perihelion, it is essential that before the first of the three conditions is addressed, the orbits be integrated to a new osculation epoch chosen near aphelion to make the simulation procedure tractable.

The line of intersection is obviously close to the lines of apsides of the two lobes, as their longitudes and latitudes of perihelion in AD 363 were very similar, $282^\circ.35$ and $+35^\circ.43$ for Lobe I and $283^\circ.05$ and $+35^\circ.27$ for Lobe II. To find the line of intersection is straightforward. In the ecliptic coordinate system, the unit vector \mathbf{R} normal to the orbital plane of a comet is a function of the longitude of the ascending node, Ω , and the orbital inclination, i :

$$\mathbf{R} = \begin{pmatrix} R_x \\ R_y \\ R_z \end{pmatrix} = \begin{pmatrix} \sin \Omega \sin i \\ -\cos \Omega \sin i \\ \cos i \end{pmatrix}. \quad (42)$$

Referring to the vector normal to the orbit of Lobe I as $\mathbf{R}(\text{I}) = [R_x(\text{I}), R_y(\text{I}), R_z(\text{I})]$, and to the orbit of Lobe II as $\mathbf{R}(\text{II}) = [R_x(\text{II}), R_y(\text{II}), R_z(\text{II})]$, a vector along the line of intersection, $\mathbf{L} = (L_x, L_y, L_z)$ is given by their vector product:

$$\mathbf{L} = \mathbf{R}(\text{I}) \times \mathbf{R}(\text{II}), \quad (43)$$

so that

$$\begin{aligned} L_x &= \begin{vmatrix} R_y(\text{I}) & R_z(\text{I}) \\ R_y(\text{II}) & R_z(\text{II}) \end{vmatrix}, \\ L_y &= \begin{vmatrix} R_z(\text{I}) & R_x(\text{I}) \\ R_z(\text{II}) & R_x(\text{II}) \end{vmatrix}, \\ L_z &= \begin{vmatrix} R_x(\text{I}) & R_y(\text{I}) \\ R_x(\text{II}) & R_y(\text{II}) \end{vmatrix}. \end{aligned} \quad (44)$$

Inserted into the equations for the position, one can use any two coordinates to calculate the true anomaly, u , of either lobe's position on the line of intersection. For Lobe I, for example, $u = u_{\text{I}}$ and

$$\begin{pmatrix} L_x \\ L_y \\ L_z \end{pmatrix} = c_0 \begin{pmatrix} P_x(\text{I}) & Q_x(\text{I}) \\ P_y(\text{I}) & Q_y(\text{I}) \\ P_z(\text{I}) & Q_z(\text{I}) \end{pmatrix} \times \begin{pmatrix} \cos u_{\text{I}} \\ \sin u_{\text{I}} \end{pmatrix}, \quad (45)$$

where c_0 is a constant and P_x, \dots, Q_z are the components, in the ecliptic coordinate system, of the unit vectors: \mathbf{P} pointing to perihelion and \mathbf{Q} 90° ahead of \mathbf{P}

Table 15
Orbital Periods of Fragments Separating From Lobe I or Lobe II at or Near Perihelion in AD 363

Fragmentation distance r_{frg}	Center-of-mass shift $\Delta U_{p \rightarrow f}(r_{\text{frg}})$ (km)	Orbital period, P_{frg} (yr)	
		Lobe I	Lobe II
q	-15	367	554
	-30	291	427
	-45	156	342
$2q$	-15	611	698
	-30	505	644
	-45	427	596

in the orbital plane in the direction of motion. The components are functions of the angular orbital elements:

$$\begin{pmatrix} P_x & Q_x \\ P_y & Q_y \\ P_z & Q_z \end{pmatrix} = \begin{pmatrix} \cos \Omega & -\sin \Omega & 0 \\ \sin \Omega & \cos \Omega & 0 \\ 0 & 0 & 1 \end{pmatrix} \times \begin{pmatrix} \cos \omega & -\sin \omega \\ \sin \omega \cos i & \cos \omega \cos i \\ \sin \omega \sin i & \cos \omega \sin i \end{pmatrix}. \quad (46)$$

Combining in (45), the expressions for, say, L_x and L_y , we get for the true anomaly of the line of intersection in the orbit of Lobe I

$$\tan u_{\text{I}} = \frac{L_x P_y(\text{I}) - L_y P_x(\text{I})}{L_y Q_x(\text{I}) - L_x Q_y(\text{I})}. \quad (47)$$

Since the position is near aphelion, one has to add 180° to the value obtained from (47) when the tangent is negative (pre-aphelion location), or subtract 180° when it is positive (post-aphelion location). This true anomaly gives the barycentric distance and time of Lobe I on the line of intersection. The same procedure provides the same data for Lobe II.

We next used the elements from Table 14 to determine the position of the line of intersection of the orbital planes of the lobes. We first integrated their motions from perihelion in AD 363 to the previous aphelion and converted the heliocentric system to the barycentric system. For an osculation epoch at the end of 5 BC, the two orbits and the gap between them are shown in Table 17. The ecliptic components of the unit vectors $\mathbf{R}(\text{I})$, $\mathbf{R}(\text{II})$, \mathbf{L} , and the lobes' true anomalies, u_{I} , u_{II} , and barycentric distances, r_{I} , r_{II} , are summarized in Table 18. The angle between the orbital planes was $13^\circ.23$, while the line of intersection made angles of $0^\circ.2$ and $0^\circ.4$ with the lines of apsides of Lobe I and Lobe II, respectively.

Table 16
Some Potential Historical Kreutz Sungrazers from 7th–11th Centuries as Possible Fragments Separating from Lobe I or Lobe II at Perihelion in AD 363

Potential Kreutz comet	Implied orbital period (yr)	Shift $\Delta U_{p \rightarrow f}(q)$ (km)	
		Lobe I	Lobe II
607	243.3	-27.3	(-72.8)
852	488.3	-8.2	-22.0
943	579.9	-4.7	-12.6
1034	670.8	-2.1	-5.5

Table 17
Adopted Sets of Barycentric Orbital Elements for Lobe I and Lobe II at Aphelion
Previous to AD 363 from Orbits in Table 14 (Equinox J2000)

Orbital element	L o b e I	L o b e II	Gap: II–I
Osculation epoch (TT)	–4 Dec 30.0	–4 Dec 30.0
Perihelion time (TT)	363 Nov 14.745	363 Nov 14.749
Argument of perihelion	80°.6143	63°.7486	–16°.8657
Longitude of ascending node	0°.8109	340°.2642	–20°.5467
Orbit inclination	144°.0694	139°.9866	–4°.0828
Perihelion distance (AU)	0.005 117 79	0.008 452 15	+0.003 334 36
Orbit eccentricity	0.999 937 18	0.999 896 25	–0.000 040 93
Reciprocal semimajor axis (AU ^{–1})	+0.012 274 54	+0.012 274 54
Orbital period (yr)	734.85	734.85

Under rigorous conditions, it would next be a matter of iteration to bring first the barycentric distances and then the times into harmony. One possible approach would be to keep these two quantities constant for one lobe, to select this time as the osculation epoch, and to iterate these quantities for the other lobe: the barycentric distance by varying ΔU of the pre-363 orbit, the time by shifting the perihelion time in AD 363.

For two reasons we did not pursue this line of attack. One reason was the tiny angles between the positions of the line of intersection of the lobes’ orbital planes and the lines of apsides, which indicated — given the approximations involved — that, angularly, the point of fragmentation was virtually indistinguishable from aphelion. The other reason was that, in the context of the proposed contact-binary model, both lobes were believed to have undergone, before reaching their perihelion in AD 363, events of secondary fragmentation, which were bound to modify, however slightly, the positions of their orbital planes and thereby introduce additional uncertainties into the orbit computations. Instead, we *assumed* that the breakup of the progenitor into the two lobes occurred at aphelion and that Lobe I began to move in an orbit described by the set of elements listed for it in Table 17. This provided us with an opportunity to simulate effects by the separation velocity (Section 7.3).

7.3. Orbit of Progenitor Prior to Fragmentation and Separation Velocities of the Lobes

Let at the adopted fragmentation time of –4 Dec 30, $\mathbf{U}_I = (x_I, y_I, z_I)$ and $\mathbf{V}_I = (\dot{x}_I, \dot{y}_I, \dot{z}_I)$ be, respectively, the orbital-position and orbital-velocity vectors of Lobe I; and let $\mathbf{U}_{II} = (x_{II}, y_{II}, z_{II})$ and $\mathbf{V}_{II} = (\dot{x}_{II}, \dot{y}_{II}, \dot{z}_{II})$ be the orbital-position and orbital-velocity vectors of Lobe II. Whereas the two position vectors were equal (neglecting the lobes’ dimensions), the velocity vectors were not. Following Figure 5, the progenitor’s orbit was fully described by the position vector \mathbf{U}_{par} and the velocity vector \mathbf{V}_{par} , an average of the velocity vectors of the lobes. In the ecliptic coordinate system,

$$\begin{aligned} \mathbf{U}_{\text{par}} &= \mathbf{U}_I = \mathbf{U}_{II} = (x_{\text{par}}, y_{\text{par}}, z_{\text{par}}) \\ \mathbf{V}_{\text{par}} &= \frac{1}{2} (\mathbf{V}_I + \mathbf{V}_{II}) = (\dot{x}_{\text{par}}, \dot{y}_{\text{par}}, \dot{z}_{\text{par}}). \end{aligned} \quad (48)$$

By integrating these position and velocity vectors from the osculation epoch back in time, the progenitor’s orbit at the previous perihelion could readily be determined.

The derivation of the progenitor’s velocity by averaging the lobes’ velocities implied that the fragments parted at equal rates in the exactly opposite directions, as depicted in Figure 5. The differences between the lobes’ orbital velocities and the velocity of the progenitor were the lobes’ *separation velocities*:

$$\begin{aligned} \mathbf{V}_{\text{sep}}(\text{I}) &= \mathbf{V}_{\text{sep}} = (\dot{x}_I - \dot{x}_{\text{par}}, \dot{y}_I - \dot{y}_{\text{par}}, \dot{z}_I - \dot{z}_{\text{par}}) \\ \mathbf{V}_{\text{sep}}(\text{II}) &= -\mathbf{V}_{\text{sep}} = (\dot{x}_{II} - \dot{x}_{\text{par}}, \dot{y}_{II} - \dot{y}_{\text{par}}, \dot{z}_{II} - \dot{z}_{\text{par}}). \end{aligned} \quad (49)$$

Given that the investigation of the separation-velocity vector was conducted in the coordinate system of RTN (radial-transverse-normal), rotating with the comet along its orbit, it was first necessary to convert the vector’s components into the ecliptic system. Writing V_R for the radial, V_T for the transverse, and V_N for the normal component of the separation velocity of Lobe I relative to the parent and $\dot{x}_{\text{sep}} = \dot{x}_I - \dot{x}_{\text{par}}$, etc., for its ecliptic components, the transformation formulas were:

$$\begin{aligned} \begin{pmatrix} \dot{x}_{\text{sep}} \\ \dot{y}_{\text{sep}} \\ \dot{z}_{\text{sep}} \end{pmatrix} &= \begin{pmatrix} P_x(\text{I}) & Q_x(\text{I}) & R_x(\text{I}) \\ P_y(\text{I}) & Q_y(\text{I}) & R_y(\text{I}) \\ P_z(\text{I}) & Q_z(\text{I}) & R_z(\text{I}) \end{pmatrix} \\ &\times \begin{pmatrix} \cos u_I & -\sin u_I & 0 \\ \sin u_I & \cos u_I & 0 \\ 0 & 0 & 1 \end{pmatrix} \times \begin{pmatrix} V_R \\ V_T \\ V_N \end{pmatrix}. \end{aligned} \quad (50)$$

From the separation velocity \dot{x}_{sep} , etc., of Lobe I relative to the parent, the components of the parent’s orbital velocity at the time of fragmentation equaled $\dot{x}_{\text{par}} = \dot{x}_I - \dot{x}_{\text{sep}}$, etc., and the components of the orbital velocity of Lobe II equaled $\dot{x}_{II} = \dot{x}_I - 2\dot{x}_{\text{sep}}$, etc.

Table 18
Line of Intersection and Lobes’ Positions

Quantity	L o b e I	L o b e II
$R_x(\text{I}), R_x(\text{II})$	+0.008 304 04	–0.217 119 35
$R_y(\text{I}), R_y(\text{II})$	–0.586 746 51	–0.605 198 22
$R_z(\text{I}), R_z(\text{II})$	–0.809 728 08	–0.765 894 44
L_x	–0.177 669 37	
L_y	+0.796 006 29	
L_z	–0.578 625 60	
u_I, u_{II}	+179°.8079	–179°.5996
r_I, r_{II} (AU)	149.55	131.89

We were now ready to simulate the orbital conditions at the *primary fragmentation event that gave birth to the Kreutz system*: At aphelion, on -4 December 30, Aristotle's comet, modeled as a bilobed rotating object, was to split into two fragments (lobes) that were to end up in the orbits presented in Tables 14 and 17.¹³ The goal was to fit, as closely as possible, the orbits of Lobes I and II in AD 363 and 5 BC as products of the contact-binary parent's pre-fragmentation orbit by determining the differential momenta (expressed in terms of the separation velocity vectors) that Lobes I and II acquired (in the opposite directions) at the breakup.

In the case of the parent's orbit being unknown, the problem could equivalently be addressed by starting from the orbit of one lobe — say, Lobe I — and by searching for a separation velocity vector \mathbf{V}_{sep} [see (49)], such that its subtraction from the lobe's orbital-velocity vector determined the parent's orbit, and its another subtraction approximated the orbit of the other lobe — Lobe II — at perihelion in AD 363 (Table 14). When successful, this exercise demonstrates that the forthright splitting of the progenitor into the two lobes is compatible with their orbital properties.

To assure that the fragments arrived at their perihelion in AD 363 in fairly tight formation (within days of one another, thereby seen simultaneously), we set $V_R = 0$, in line with Papers 1 and 2. We began to address the task by adopting for the other two separation velocity components of Lobe I the values from Table 6 of Paper 2, $V_T = -1.86 \text{ m s}^{-1}$ and $V_N = -1.80 \text{ m s}^{-1}$. These velocities had of course been derived from the 19th-century osculating orbits of the 1843 and 1882 sungrazers, thereby ignoring all time dependent effects, including the two-millenia long, continuous planetary perturbations of the two sungrazers and their precursors.

Contrary to the arguments associated with the quest to explain the orbital differences among Kreutz sungrazers (and especially the discrete populations) by a cumulative effect of the planetary perturbations over longer periods of time, our results show that the gaps between the orbital elements of the two lobes, or equivalently, the 1843 and 1882 sungrazers, were being *contracted* with time. Indeed, while the difference between the inclinations in the 4th century was about 4° , it was reduced to less than $2^\circ.5$ in the 19th century; similarly, in the same period of time the difference in the longitude of the ascending node dropped from more than 21° to 16° , and the difference in the perihelion distance from $0.7 R_\odot$ to $0.5 R_\odot$. These systematic trends manifestly demonstrate that the planetary perturbations could not possibly account for the existence of the Kreutz system's populations.

The diminishing differences between the orbital elements of the two giant sungrazers intervened in our efforts to simulate the initial magnitude of the separation velocity between the lobes in that the numbers based on the 19th century orbits turned out to have been much too low. It was necessary to iterate the orbital solution, with the result showing eventually that the transverse component of the separation velocity was about 26 percent higher and the normal component 54 percent higher than estimated in Paper 2.

¹³ A possible independent separation of the neck was not simulated in this exercise.

The outcome of our computer simulations of the birth of the two most massive fragments of the Kreutz system as products of the bilobed progenitor's splitting is presented in Tables 19 and 20. Although we made no effort to strictly optimize the solution, we found that at the adopted fragmentation time of -4 December 30.0 TT, essentially the point of aphelion, either lobe separated with a velocity, relative to the progenitor's center of mass, of

$$|\mathbf{V}_{\text{sep}}| = 3.63 \text{ m s}^{-1}. \quad (51)$$

The transverse and normal components of the separation velocity of Lobe I were, respectively, $V_T(t) = -2.35 \text{ m s}^{-1}$ and $V_N(t) = -2.77 \text{ m s}^{-1}$; the radial component, as already noted, was forced to be nil. Thanks to this condition, Lobe II — whose transverse and normal components of the separation velocity were of the same magnitude, but of the opposite sign — reached its perihelion in AD 363 only about 4.2 days after Lobe I. If the radial component were not nil — or close to nil — the two lobes would have arrived at perihelion weeks, possibly months, apart and they would not have been perceived as an essentially single event, contrary to the impression that one gets from the Roman historian's account.

We note that even though the gaps between the orbital elements of the two lobes (Table 17) were greater than between the osculating orbits of the 1843 and 1882 sungrazers, the separation velocity that accounts for the gaps is still low. Interpreting it as the progenitor's rotation velocity, we could estimate the compatible rotation period. If either lobe is assumed to be about 50 km in diameter, so is the distance between the centers of mass. If the circumference, $2\pi \cdot 50 = 314 \text{ km}$, is described in one day, this equals 3.63 m s^{-1} , derived in (51). The rotation period of 24 hr is rather on the long side.

The 4-day gap between the perihelion times of the two lobes is no surprise. In Paper 2 we anticipated a gap of 2.9 days with a lower separation velocity, showing that the gap is an effect of the transverse component. The standard time of 363 Nov 15.0 TT that we have used throughout this paper in search of the various orbital solutions was essentially a default value, dictated by the narrative on the observation of the daylight comets. We could have used another date nearby with the virtually identical outcome. Indeed, a change in Lobe I's orbital period of one month between AD 363 and 1106 is triggered by a radial shift in the center-of-mass position of only 1.7 meters at perihelion, a trivial effect.

Either lobe is believed to have undergone events of secondary fragmentation not long after their birth. According to the model in Paper 2, Lobe I was likely to have produced the precursors of Populations Pre-I and Pe, respectively, whereas Lobe II was apparently the parent to Fragment IIa and Precursor IIa*. In the light of these events, the agreement in Table 19 between the orbital elements of Lobe II at the AD 363 and 5 BC epochs derived from the back integration of the precursor orbit of the Great September Comet of 1882 on the one hand and from the precursor orbit of the Great March Comet of 1843 and the fragmentation parameters of the progenitor on the other hand is astonishingly good. The high degree of correspondence demonstrates in the very least the feasibility — and in fact fundamental veracity — of the proposed fragmentation hypothesis.

Table 19
Sets of Orbital Elements for Lobe II (Heliocentric in AD 363, Barycentric in 5 BC) Derived From Orbit of Lobe I and Fragmentation Parameters (Equinox J2000)

Orbital element	Heliocentric orbit in AD 363		Barycentric orbit in 5 BC	
	Lobe II	Difference ^a	Lobe II	Difference ^b
Osculation epoch (TT)	363 Dec 24.0	-4 Dec 30.0
Perihelion time (TT)	363 Nov 19.178	+4.178	363 Nov 18.923	+3.923
Argument of perihelion	65°.2762	+0°.3567	64°.1015	+0°.3529
Longitude of ascending node	341°.4695	-0°.3002	339°.9582	-0°.3060
Orbit inclination	140°.3356	-0°.0515	139°.9406	-0°.0460
Perihelion distance (AU)	0.008 498 24	+0.000 051 90	0.008 506 16	+0.000 054 01
Orbit eccentricity	0.999 898 00	-0.000 000 56	0.999 895 39	-0.000 000 66
Reciprocal semimajor axis (AU ⁻¹)	+0.012 001 91	-0.000 007 83	+0.012 274 29	-0.000 000 25
Orbital period (yr)	760.54	+0.74	734.88	+0.03
Separation velocity of Lobe II from parent:	$V_{\text{sep}} = 3.63 \text{ m s}^{-1}$ $V_{\text{R}} = 0.00$ (assumed)		$V_{\text{T}} = +2.35 \text{ m s}^{-1}$ $V_{\text{N}} = +2.77 \text{ m s}^{-1}$	

Notes.

^a Difference between the value of the orbital element in column 2 minus the value of the equivalent element in column 4 of Table 14 (Lobe II).

^b Difference between the value of the orbital element in column 4 minus the value of the equivalent element in column 3 of Table 17 (Lobe II).

Another major conclusion is that Aristotle’s comet, which according to historical accounts appeared in the winter at the end of 373 BC or the beginning of 372 BC, fits our orbit simulation scheme as the putative contact-binary progenitor. We no longer see any reason to doubt this object’s significance in regard to the Kreutz system. We integrated the orbit of the progenitor back in time over two revolutions about the Sun, showing the result in Table 20. It is perhaps somewhat surprising to see the orbit of Aristotle’s comet resembling the orbit of the Great September Comet of 1882 in both the angular elements and the period, with only the perihelion distance deviating a little toward that of the 1843 sungrazer.

Several accounts of historical comets in Hasegawa’s (1980) catalog between 1141 BC and 1201 BC (recorded in Babylonia, Greece, Troy, and Assyria) and another object between 1921 BC and 1950 BC (recorded in Chaldea)¹⁴ — most copied from Pingré’s (1783) cometography — led us to integrate the orbit from 372 BC back in time over two revolutions about the Sun. While we felt that there was no point in deriving ΔU shifts to bring the computed perihelion times into better agreement with the recorded times, it is clear that the differences of not more than several decades would require fairly minor values of the shift corrections. One cannot rule out that especially the Greek comet seen either in 1176 or 1201 BC and the one in the 20th century BC could have been previous appearances of Aristotle’s comet.

The somewhat longer than expected period of time between Aristotle’s comet and the candidate objects in the late 12th century BC is not surprising, if some of the 16 comets in Hasegawa’s catalog between 532 and 394 BC were siblings of Aristotle’s comet whose birth dated back to the 12th century BC. Although speculative, this argument is supported by six Kreutz candidates on Hasegawa & Nakano’s (2001) list between AD 101 and 252, potentially their next returns to perihelion.

¹⁴ Observations must have been made near the end of the Sumerian era; Chaldea existed in the same region about a millennium or more later.

The agreement between the predicted perihelion time of Aristotle’s comet and the alleged appearance of the Sumerian comet, to better than 50 years is excellent given the poor dating of those times. It suffices to mention that the difference between two historical scales, the so-called short and middle chronologies, is 64 years.

In any case, the Kreutz sungrazer system in our terminology refers to fragments that were derived from either Lobe I or Lobe II (or the neck, if it ever established its own hierarchy of products) at or after the breakup of Aristotle’s comet into the lobes at large heliocentric distance about two millennia ago. Any sungrazers that were given birth in the course of previous fragmentation events involving Aristotle’s comet or its predecessor, during which the object’s contact-binary nature remained intact, are obviously related to the Kreutz sungrazers by virtue of being derived from the common parent, but they stay outside our area of interest.

8. COMMENTS ON POTENTIAL ORBITAL HISTORY OF SUNGRAZING COMET PEREYRA

Next to the fragments of the Great September Comet of 1882 and comet Ikeya-Seki, Pereyra (C/1963 R1) is the only other major Kreutz sungrazer whose orbital period is known with relatively high accuracy.¹⁵ Pereyra’s osculating orbit (Marsden 1967, Marsden et al. 1978) was classified by Marsden as Population (or Subgroup) I, even though it does not resemble the orbit of the 1843 sungrazer as closely as does, for example, the Great Southern Comet of 1880 (C/1880 C1). The notable difference is in the perihelion distance, which is about 10 percent smaller and treacherously close to the Sun’s radius. Also, Pereyra’s orbital period of 900 yr is longer than for any other bright Kreutz sungrazer with a known period. Although the comet was observed exclusively after perihelion,¹⁶ the derived orbital period is deemed relevant

¹⁵ Comet Lovejoy (C/2011 W3), whose orbital period has also been determined rather accurately (Sekanina & Chodas 2012), disintegrated shortly after perihelion and we do not rank it as a major Kreutz sungrazer.

¹⁶ The comet was discovered three weeks after perihelion.

Table 20
Sets of Predicted Orbital Elements for Aristotle’s Comet Between 5 BC and 1901 BC (Equinox J2000)

Orbital element	Aphelion: 5 BC (barycentric)	Perihelion: 372 BC (heliocentric)	Perihelion: 1125 BC (heliocentric)	Perihelion: 1901 BC (heliocentric)
Osculation epoch (TT)	−4 Dec 30.0	−371 Jan 11.0	−1124 Nov 20.0	−1900 Feb 8.0
Perihelion time (TT)	−372 Dec 30.5	−372 Dec 30.1	−1124 Oct 26.4	−1900 Jan 3.8
Argument of perihelion	70°.8125	68°.3540	67°.2895	66°.0865
Longitude of ascending node	348°.5772	345°.4348	344°.0560	342°.3441
Orbit inclination	142°.1932	141°.3247	141°.0673	140°.5414
Perihelion distance (AU)	0.006 614 77	0.006 800 71	0.006 824 15	0.006 774 65
Orbit eccentricity	0.999 918 81	0.999 920 33	0.999 920 42	0.999 921 79
Reciprocal semimajor axis (AU ^{−1})	+0.012 274 43	+0.011 715 37	+0.011 660 75	+0.011 545 07
Orbital period (yr)	734.86	788.61	794.16	806.13

to the comet’s preperihelion motion because its nucleus apparently did not fragment.¹⁷

The odd orbital properties make Pereyra’s comet a maverick that is difficult to compartmentalize among the bright Kreutz sungrazers. The long orbital period is particularly perplexing because it suggests the previous perihelion about 50 years prior to the 1106 comet. Marsden wrestled with the problem, noting an agreement between the orbits of the 1843 and 1880 sungrazers at their previous return to perihelion when he assigned an orbital period near 370 yr to the former— about one half the period we adopt — and slightly over 400 yr to the latter. He combined the evolution of this pair with that of comet Pereyra, whose orbital period was more than twice as long. The solutions that Marsden deemed the most promising required that the parent — which he called the “Combo” — should have passed perihelion either in mid-February 1072 when Pereyra separated and in mid-March 1463 when the 1880 comet separated from the 1843 comet; or in early December 1114 when Pereyra separated and in late October 1487 for the second fragmentation event. The second solution — the more probable one according to Marsden — implied for Pereyra a barycentric orbital period of 849 yr, which was by nearly 60 yr shorter than the most probable value. As Marsden himself noted, no sungrazer was observed in either 1463 or 1487. One may add that none was seen in 1072 or 1114 either (see England 2002). Not to mention that a subsequent revision of the orbit of the 1843 sungrazer (Sekanina & Chodas 2008) ruled out the possibility of its orbital period having been anywhere near 400 yr.

We have now revisited the issue of Pereyra’s sungrazer by first computing the time of its previous perihelion, based on Marsden’s osculating elements. Our orbit integration showed that the perihelion time should have occurred on 1057 April 7, so that its barycentric orbital period was 906.4 yr. Marsden determined the orbital period with a mean error of ± 17 yr. Accordingly, a perihelion passage between the years 1040 and 1074 should satisfy the predicted perihelion time within $\pm 1\sigma$.

¹⁷ Roemer (1963, 1965) reported a possible secondary nucleus 0’.1 from the primary on 1963 November 9, nearly 80 days after perihelion, which was never confirmed. Its existence is highly unlikely, because a genuine companion (i) should have been detected much earlier and (ii) this long after perihelion the separation distance from the primary should have been substantially greater.

Hasegawa & Nakano (2001) have on their list of potential Kreutz sungrazers an exceedingly bright Chinese-Korean comet, allegedly of absolute magnitude -1 , which was to pass perihelion nominally on 1041 August 4. The historical records noted that the comet was first seen on 1041 September 1. We propose that Pereyra’s comet separated from this parent at its 1041 return to perihelion and examine the ramifications of this hypothesis.

We integrated the gravitational orbit of Pereyra’s comet, adjusted to fit the perihelion of the 1041 comet, and found that its previous perihelion would have occurred on 158 November 11. While Hasegawa & Nakano tabulate a possible Kreutz comet in January 133 and another one in October 191, we prefer a linkage to Lobe I in November 363, so that Pereyra would be its indirect, second-generation product.

Table 21 shows that the proposed history of Pereyra’s comet is entirely feasible. A notable feature is a rapid rotation of the orbital plane: between 1041 and 363 the nodal line advanced at an incredible rate of more than 8° per revolution. The sudden jump in the orbital period of more than 200 yr was triggered by a radial shift of the center of mass by less than 4 km at the 1041 perihelion, when the comet was barely 40,000 km above the photosphere. The orbital elements at perihelion in AD 363 show that Pereyra’s precursor obviously separated from Lobe I, as predicted in Papers 1 and 2, where it was referred to as Fragment Pe. The differences in the elements relative to Lobe I are, however, much smaller than the differences between Lobes I and II. For example, the gap in the nodal longitude is 7° compared to 21° , in the inclination $0^\circ.8$ compared to $3^\circ.8$, and the perihelion distance $0.04 R_\odot$ compared to $0.7 R_\odot$.

Even though the gaps between the 363 orbital elements of Lobe I and Pereyra’s precursor were much smaller than between those of Lobes I and II, they were large enough that obviously the precursor arrived at perihelion in AD 363 as a separate fragment and that instead of Lobe I’s path from the apparition of 363 to 1106 it followed an alternative path to 1041. In other words, unlike for other Population I fragments (such as C/1880 C1), the orbital evolution of Pereyra became divorced from that population’s parent already before the first passage through perihelion. This explains why comet Pereyra was among Population I members a maverick: it was their sibling, but a more distant sibling.

Table 21

Fragmentation Scenario Based Gravitational Solution for Comet Pereyra Returns of 1963, 1041, and 363 (Equinox J2000)

Orbital element	Perihelion: 1963	Perihelion: 1041	Perihelion: 363
Osculation epoch (TT)	1963 Sept 8.0	1041 Aug 26.0	363 Dec 24.0
Perihelion time (TT)	1963 Aug 23.95638	1041 Aug 4.0	363 Nov 15.0
Argument of perihelion	86°.1602	82°.9111	76°.2557
Longitude of ascending node	7°.9392	3°.8349	355°.7448
Orbit inclination	144°.5821	144°.3115	143°.4177
Perihelion distance (AU)	0.005 064 90	0.004 911 14	0.004 995 22
Orbit eccentricity	0.999 946 41	0.999 939 31	0.999 939 34
Reciprocal semimajor axis (AU ⁻¹)	+0.010 579 57	+0.012 356 59	+0.012 144 13
Orbital period (yr)	918.96	728.03	747.22
Center-of-mass shift $\Delta U_{p \rightarrow f}(r_{\text{frg}})$ (km)		+3.7817	
Fragmentation distance r_{frg}		perihelion	

The reader may notice a remarkable similarity in the time of the year between the arrivals of the 1041 comet and the 1138 comet. The adopted perihelion dates differ by three days, the date of the first observation by two days. The length of the period of observation of the 1041 comet is disputed: the quoted Chinese source says more than 90 days, while the Korean source says “20 and some odd days,” a little less than for the 1138 comet. A large uncertainty was obviously involved. The observations of the 1138 comet were terminated, in part, because of interference from moonlight, when the predicted apparent magnitude was 4; after the observing conditions improved, there evidently was nobody to pick up the comet again. It seems that this happened with the 1041 comet in Korea as well, given that the Moon phases were moved forward one week in 1041 compared to 1138. Unlike the Koreans, the Chinese must have observed the *tail* of the 1041 comet until its head was of apparent magnitude ~ 7 , as prominent sungrazers sometimes have been (see Paper 2). In any case, the head of the 1041 comet could not possibly have been of an absolute magnitude of -1 . Adopting for this object the same post-perihelion rate of fading as for the 1138 comet, apparent magnitude 7 at the end of November 1041 gives with Hasegawa & Nakano’s ephemeris the post-perihelion absolute magnitude $H_0^+ = 1.7$ and, with the comet’s perihelion distance of 0.00491 AU, its preperihelion absolute magnitude becomes $H_0^- = 4.0$, or about 1.2 mag fainter than we have assigned to the 1138 comet.

9. ARISTOTLE’S COMET: WHY A CONTACT BINARY AND WHY APHELION BREAKUP?

Besides the arguments favoring the idea of a contact-binary model for the progenitor that rely on the intrinsic properties of the Kreutz system and have been presented in Paper 1, this paradigm is likewise supported by independent circumstantial evidence. Among the six comets imaged at closeup by cameras on board spacecraft (1P/Halley, 19P/Borrelly, 81P/Wild, 9P/Tempel, 103P/Hartley, 67P/Churyumov-Gerasimenko) and one by radar (8P/Tuttle), the nuclei of at least two (8P, 67P) were found to be bilobed, while the nuclei of 103P (described as peanut-shaped) and perhaps even 1P and 19P had similar outlines (e.g., Harmon et al. 2010, A’Hearn et al. 2011, Jutzi & Asphaug 2015, Jorda et al. 2016).

Another line of evidence that generally corroborates the contact-binary model is the existence of *persisting* twin objects both among short-period comets (such as 3D/Biela, observed double at two consecutive returns to perihelion) and among comets of longer period (such as the pair of C/2002 A1 and C/2002 A2, both under observation over more than two years) as well as among the Kuiper Belt objects (e.g., Goldreich et al. 2002), including the Pluto–Charon pair.

Discovered several years ago, the Kuiper Belt object (486958) Arrokoth = 2014 MU₆₉ (a.k.a. Ultima Thule) was imaged by the New Horizons Mission (Stern et al. 2019), offering arguably the most robust piece of supporting circumstantial evidence for at least two reasons: (i) the overall length of this contact-binary object equaled, according to Stern et al., 36 km and the larger, highly-flattened lobe’s maximum diameter was 22 km, comparable to the crudely estimated dimensions of the Great September Comet of 1882 (Sekanina 2002), a major surviving mass of the presumed Kreutz progenitor; and (ii) the likelihood that contact binaries like Arrokoth are common among transneptunian objects in general and Kuiper Belt objects in particular, a notion expressed independently by several researchers (e.g., Rickman et al. 2015, Stern et al. 2019, Benecchi et al. 2019). Contact-binary objects are believed to have initially been separate objects orbiting about one another at very low velocities (a few meters per second), eventually collapsing gravitationally into a single body (e.g., Stern et al. 2019, Grundy et al. 2020, McKinnon et al. 2020).

Extending this rationale to its seemingly logical conclusion, one would argue that the Kreutz progenitor was a Kuiper Belt object. Unfortunately, since Kuiper Belt objects are not perturbed into retrograde orbits, this hypothesis has to be abandoned. Instead, a plausible region of origin could be the inner Oort Cloud, the source of Halley-type comets (Levison et al. 2001). Inner Oort Cloud objects may have an affinity for forming contact binaries like Kuiper Belt objects, although the lower spatial density offers a less favorable environment. Once the progenitor enters — presumably thanks to mostly indirect perturbations by the outer planets, Jupiter in particular — an orbit that is inclined 90° to 100° to the ecliptic and has an orbital period of ~ 800 yr and perihelion distance of less than 2 AU, a process of migration

governed by continuing long-term indirect planetary perturbations was shown by Bailey et al. (1992) to have been progressively reducing the perihelion distance over a period on the order of a million years, injecting eventually the object into the observed retrograde sungrazing orbit.

Fernández et al. (2021) have recently considered three different models for the Kreutz system progenitor, concluding that the most promising one was an Oort-Cloud comet, which was first injected into an Earth-crossing orbit and then perturbed into a sungrazing orbit by the Lidov-Kozai mechanism. While this model has some attractive features, it wrestles with the problem of a rate at which such massive objects could be delivered into these orbits. The study does not address the issue of discrete populations of sungrazer fragments and deals only with near-perihelion tidally-triggered fragmentation.

There indeed is a universal consensus that the Sun's tidal forces, possibly in concert with other forces, instigate perihelion fragmentation of the Kreutz comets. One such other potential trigger is the Sun's extreme heat that foments stress because of the propagation of a thermal wave through the nucleus, unless massive amounts of ejected dust in the atmosphere make it optically thick, thereby protecting the nucleus from direct exposure. These effects are of course superposed on presumably less robust effects of the nucleus' rotation and/or precession.

This conclusion is based on a plausible premise that a nucleus breaks up, if stress in its interior, induced by the Sun tidally, and potentially exacerbated thermally, exceeds the strength of the nucleus. It is fitting to ask what happens if the *magnitude of the combined tidal, thermal, and rotational stresses does not exceed the nucleus strength*. One expects that the object then survives perihelion passage, though *not necessarily intact*: some, however minor, damage is being sustained at each close approach to the Sun and the extent of this damage adds up, revolution after revolution. Indeed, the egress of a sungrazer out of the solar corona is always anticipated with some trepidation over its survival. The observations offer only one of three answers: (i) the object emerges with a single nuclear condensation, in which case it is said to have survived; or (ii) it emerges with two or more condensations, indicating that its nucleus split; or (iii) it emerges with no condensation, the sign of disintegration. What remains hidden in the case of survival is the *extent of damage*: the observations do not discriminate between a structurally intact, nearly intact, moderately damaged, or heavily damaged (but still unbroken) nucleus.

Although hidden to the observers, the genuine physical condition of the nucleus at the end of its extremely close approach to the Sun's photosphere makes all the difference in the comet's future life. An intact or nearly intact object is obviously much more likely to successfully complete the hundreds-of-years lasting revolution about the Sun than an object that barely held together at the start of the long journey. The gradual weakening of structural cohesion of a piece of material under terrestrial conditions (on vastly shorter time scales) is known as *material fatigue*; there is no reason why the process could not apply, on another time scale, to objects in space as well.

When the celestial object is a contact binary, the neck is likely to be more susceptible to damage than the lobes. In general, the neck is subjected to either compressive or tensile stress, depending on the size and mass

(and thus the density) of the lobes as well as the rate of rotation. The magnitude of the force also depends on the cross-sectional area of the neck. For Arrokoth, McKinnon et al. (2020) determined that the neck was being subjected to compression if the object's density was greater than 0.25 g cm^{-3} , which was likely to be the case. Judging from the estimated giant size of the nucleus of C/1882 R1, the neck of the proposed Kreutz progenitor should have been subjected to an even higher level of compressive stress, unless the rotation was much faster than Arrokoth's.

Except in the Sun's proximity, the force affecting the Kreutz progenitor's neck should not have changed materially over the period of time from the instance of gentle merger of the two lobes until after the process of the object's slow migration into the sungrazing orbit was long underway. Bailey et al.'s (1992) computations suggest that the perihelion distance had dropped to $\sim 0.1 \text{ AU}$ approximately 50 revolutions and to $\sim 0.01 \text{ AU}$ some 25 revolutions about the Sun before the minimum distance was reached. While the object was repeatedly — every 700–800 years or so — approaching the Sun in an orbit whose perihelion distance followed this downward spiral, the near-perihelion environment was subjecting the neck to three *cyclic* effects that were gradually accumulating from orbit to orbit and, as a result, weakening the bond between the pair of lobes: two such effects, as already noted, were, respectively, tensile stress, prompted by the Sun's tidal force, and thermal stress, triggered by an enormous heat pulse, both strongly perihelion-distance dependent; a third was an imprint of similarly varying rates of vigorous sublimation of volatile substances from the neck, thereby reducing its cross-sectional area with time.

The neck of the bilobed Kreutz progenitor is thus presumed to have been subjected to an essentially constant load, with dozens of overlapping *cyclic* stress peaks centered, once every 700–800 years, on the time of perihelion, the magnitude of which was growing progressively from orbit to next orbit as the perihelion distance was steadily decreasing toward the presumed present value slightly exceeding $1 R_{\odot}$. It is this cyclic component of the load that represents what one can refer to as an extreme case of the already noted material fatigue, even though the duration of the cycle is vastly longer and the number of cycles orders of magnitude lower than in applications to fabricated materials, metals in particular, under usual terrestrial conditions.

In summary, fatigue of material is a process of progressive, localized deformation and/or weakening in an object subjected to a cyclic load below the static material strength, which prompts the development, growth, and propagation of cracks from cycle to cycle, culminating in the object's fracture, a.k.a. fatigue failure (see, e.g., Suresh 2014). Since fatigue is an irreversible stochastic process with a degree of randomness, the lifetime, defined by the number of cycles to failure, is rather poorly determined, especially in the presence of an appreciable background stress. Usually associated with tensile stresses, fatigue has several phases, but most time is consumed in the crack growth phase. Once a crack has begun, each loading cycle enlarges the crack by a small amount until it reaches a critical point when the stress intensity factor of the crack exceeds the fracture toughness of the mate-

rial producing its rapid propagation that nearly instantly completes the fracture.

Because of the limited number of orbits with perihelia very close to the Sun during the orbital evolution, the neck of the Kreutz progenitor was exposed to *low-cycle fatigue* (when the number of cycles is $\ll 10^5$). And since the location of the point of failure is essentially random in time, the location of aphelion close to 160 AU from the Sun implies that there is a ~ 50 percent chance of fracture at heliocentric distances >140 AU, a ~ 60 percent chance at >130 AU, a ~ 70 percent chance at >110 AU, and an ~ 80 percent chance at >90 AU from the Sun. Accordingly, the probability of breakup at large heliocentric distance is high.

It is noted that fragmentation events at arbitrary (and generally large) distances from the Sun coexist with events of perihelion fragmentation because of strongly heterogeneous structure and morphology of the nuclei: the former incidents are their response to an *accumulated effect of cyclic episodes of deformation, the magnitude of which is smaller than a fracture limit*, whereas the latter occurrences are their response to *discrete instances of damage whose magnitudes reach or exceed a relevant fracture limit*. Accordingly, while new damage (cracks initiation) is always inflicted over a short period of time around perihelion, the ultimate response (completed cracks propagation) may or may not be constrained to this orbital arc, depending on the magnitude of the injury. Hence, a Kreutz sungrazer may fragment at any point of the orbit, including aphelion.

10. CONCLUSIONS

In broad terms, the purpose of this paper was to conduct a feasibility study in support of the contact-binary model for the orbital history of the Kreutz sungrazer system. While the problem potentially has a large number of solutions, each of which satisfies a set of boundary conditions, our task was to demonstrate that the particular solution that we chose to pursue was one of them. Our approach was based on the assumption that the largest surviving masses of the two lobes of the contact-binary progenitor were the Great March Comet of 1843 (Lobe I) and the Great September Comet of 1882 (Lobe II), associated with Populations I and II, respectively. We accepted Marsden's (1967) result on the undisputed genetic connection of the 1882 sungrazer and Ikeya-Seki's comet, which separated from their common parent at the previous perihelion passage.

We settled the notorious, protracted dispute over the position of the Great Comet of 1106 in the hierarchy of the Kreutz system. We developed a new technique for deriving the time of the previous return of Ikeya-Seki's comet to perihelion, based on linking the 1965 preperihelion astrometric observations with the early post-perihelion ones. The evidence pointed unequivocally to the conclusion that the comet was at perihelion around the year 1139, more than three decades after the appearance of the 1106 comet. A close relationship between the 1106 comet on the one hand and Ikeya-Seki (and the 1882 sungrazer) on the other hand was thus ruled out. By contrast, we see no obstacle for accepting the 1106 comet as the previous appearance of the Great March Comet of 1843, supported by the orbital computations by Sekanina & Chodas (2008).

We also settled the other tenacious problem, previously brought up by Marsden (1989): Should there have been a second parent comet in the early 12th century to account for two populations (or subgroups) of the Kreutz sungrazers? In the case we deal with here, this presents a dilemma: Where was the parent comet of the 1882/1965 pair, if it was not the 1106 comet? Our — first ever — reference to the Chinese comet of 1138 as the pair's parent did: (i) answer the above question; (ii) show the time of its appearance consistent with the prediction from our analysis of comet Ikeya-Seki; (iii) turn out to be in excellent agreement with Marsden's (1967) prediction of the previous appearance of the 1882 sungrazer; (iv) substantially improve the orbital agreement between the 1882 sungrazer and Ikeya-Seki in comparison with Marsden's (1967) results for their assumed common origin in 1115; and (v) demonstrate that an intrinsically bright Kreutz sungrazer that was at perihelion in early August and unobserved in broad daylight, was not necessarily missed, as was often claimed in the literature.

We are rather confident that the Chinese comet of 1138 was the 12th-century "missing" major sungrazer, even though we admit that our arguments are unfortunately based on a minimum amount of data. Comparison with the naked-eye's limiting magnitude for stellar objects showed that this comet's *post-perihelion intrinsic* brightness was apparently greater than that of the 1843 sungrazer and could have been comparable to the brightness of the 1882 sungrazer. Its *apparent* brightness suffered from extremely unfavorable geometric conditions during the object's departure from perihelion on the far side of the Sun. The description of this comet (Ho 1962) is similar to the account, in a Korean source, of a suspected Kreutz sungrazer of 1041 (Hasegawa & Nakano 2001), which appeared at the same time of the year.

Two modes of orbit integration that we applied in an effort to link consecutive returns of the Kreutz sungrazers to perihelion were referred to as, respectively, a *sublimation scenario* and a *fragmentation scenario*. In the first mode the orbital period was being affected continuously by an outgassing-driven nongravitational acceleration, requiring no fragmentation. The other mode was applicable only in the presence of near-perihelion tidally-driven fragmentation, requiring no nongravitational effects; the orbital period was altered suddenly. A parent's breakup essentially along a plane perpendicular to the radius vector resulted in the generation of two or more fragments whose centers of mass were located at slightly different heliocentric distances relative to the parent's center of mass, yet at the time of breakup they had the same orbital velocity. The fragments, with no momentum exchange involved, were thus bound to end up in different orbits; the period was the longer the farther from the Sun was the center of mass. The enormity of this effect at perihelion in *sungrazing* orbits is illustrated by noting that a shift of one kilometer (a few percent of the size of a major sungrazer's nucleus) in the radial direction could easily change a 700 yr period by ~ 40 yr.

The Kreutz sungrazers are of course subjected to both modes of orbit transformation, and comet Ikeya-Seki was an example on which the interaction between them was illustrated. We showed that at the time of tidal splitting fragment B was at the sunward end of the parent nucleus and its orbital period would have been shorter than that

of the main fragment A, if it were not subjected to a significant nongravitational acceleration. Accordingly, the orbital period of the *parent* was shorter than that of fragment A. This explains why the back integration of the orbit of this fragment indicates the previous perihelion around the year 1115, while the comet actually passed perihelion (as part of its own parent comet) more than 20 years later.

We did not mix the two modes of orbit integration, the sublimation and fragmentation scenarios, in our orbit simulation computations. We demonstrated that either of them successfully linked the three returns of the largest surviving masses of Lobe I, 1843–1106–363, and Lobe II, 1882–1138–363, even though the sublimation scenario required an improbably high nongravitational acceleration to accomplish the linkage for Lobe II. The fragmentation scenario did not need center-of-mass shifts greater than a few kilometers at perihelion, deemed very modest and quite acceptable. For Lobe II we described the sequence of two fragmentation events in the year 1138: in the primary event at perihelion the arriving parent, presumed to have been more than 60 km across, shed a minor fragment into an orbit of long period, while its major fragment split tidally again, about 2.5 hr later, into the 1882 sungrazer and Ikeya-Seki's comet.

In connection with the sublimation scenario we point out that the current computer techniques, aiming to account for variations in the nongravitational acceleration whose effects are asymmetric relative to perihelion, are inadequate and need a conceptual upgrade. Refined methods should unquestionably have a favorable effect on simulating the orbital evolution of the Kreutz sungrazers in the future.

While the sublimation scenario failed to fit the sungrazers' orbital changes prior to AD 363, the fragmentation scenario — even without the benefit of incorporating any nongravitational motion — allowed us to set up a method of successfully simulating the orbits of Lobes I and II toward their point of birth, essentially at aphelion previous to the perihelion passage in AD 363. We adopted a default perihelion time of 363 Nov 15.0 (which was a convenient standard to which the arriving sungrazers' orbits were referred to rather than the actual time of perihelion passage) and computed for either lobe a fragmentation scenario based gravitational orbit that linked its perihelion time in AD 363 with the perihelion time expected for Aristotle's comet — the proposed contact-binary progenitor — in 372 BC. It turned out that the line of intersection of the orbital planes of the lobes, on which they had to be located at the time of their separation from the common parent, made such extremely small angles with the lobes' lines of apsides that the assumption of a breakup at aphelion was bound to be a very good approximation.

With this aphelion breakup of Aristotle's comet set at the very end of 5 BC at a heliocentric distance of 163 AU, we further assumed that the two lobes were of equal dimensions, separating with equal velocities in the opposite directions, and that the progenitor was spinning along an axis pointing at the Sun. The radial component of the separation velocity was then nil, while the transverse component determined the perihelion distances as well as perihelion times of the lobes and the normal component governed the spatial positions of their orbital planes. A

separation velocity of 3.63 m s^{-1} fitted the angular elements to about $0^\circ.3$, demonstrating that the existence of the two major populations of the Kreutz system as the product of fragmentation of a progenitor comet at large heliocentric distance is feasible and fundamentally correct. The procedure also resulted in a predicted set of orbital elements for Aristotle's comet.

In the light of the well-known difficulties that efforts to compartmentalize the orbital characteristics of the Kreutz comet discovered by Pereyra in 1963 had provoked in the past, we offer a novel explanation to the oddities of this maverick sungrazer. With its derived period exceeding 900 yr, a plausible previous appearance was the comet of 1041 that passed perihelion in early August according to Hasegawa & Nakano (2001), a case of interest in its own right. Integration of Pereyra's motion suggests that its precursor had separated from Lobe I already before the perihelion passage in AD 363. This circumstance allowed Pereyra's comet to bypass the normal evolutionary path for members of Population I via the Great Comet of 1106 and instead to follow an alternative path via the comet of 1041. This example illustrates the diversity of orbital tracks that the Kreutz sungrazers could heed, thus explaining the large number of discrete populations presented in Paper 1.

The Kreutz sungrazers are still believed to fragment mostly at close proximity of perihelion due to the Sun's tidal forces. This may very well be true. However, the existence of discrete populations of fragments with large gaps between their angular elements and perihelion distances cannot be a product of perihelion fragmentation, alone or enhanced with effects of the indirect planetary perturbations over periods of time that are not excessively long. We argue that the sungrazers are in fact subject to fragmentation along the entire orbit around the Sun, including aphelion, because of material fatigue of their nuclei. The perihelion region is where a Kreutz sungrazer is exposed to a cyclic load, whose magnitude is below the static material strength, yet it prompts the growth and propagation of cracks, resulting eventually in fatigue failure. This condition is reached randomly, at an arbitrary time. Since sungrazers spend most time at large heliocentric distance, fatigue fracture far from the Sun is likely. The probability for a rotating contact-binary Kreutz sungrazer may further be augmented by continuous rotation stress and the potentially brittle nature of the connecting neck.

The first author was in charge of this study's strategy, the second author was responsible for performing the orbital computations. This research was carried out in part at the Jet Propulsion Laboratory, California Institute of Technology, under contract with the National Aeronautics and Space Administration.

Appendix

KREUTZ'S ORBIT FOR PRIMARY FRAGMENT OF THE GREAT SEPTEMBER COMET OF 1882

Because the *Catalogue of Cometary Orbits* by Marsden & Williams (2008) lists for the 1882 sungrazer's primary nucleus (fragment B or No. 2) the relativistic orbit by Hufnagel (1919), Kreutz's (1891) definitive nonrelativistic

tic orbit for this fragment, converted to equinox J2000, is not widely accessible. The purpose here is to alleviate this problem. The following set of orbital elements is that published by Kreutz on page 35 of his Paper II, but updated using current conventions:

(1) Equinox 1882.0, employed by Kreutz, has been replaced by J2000.

(2) Berlin Mean Time has been converted to Universal Time by adding 12 hr and subtracting the longitude of Berlin Observatory (IAU code 548; active 1835–1913), $0^{\text{h}}53^{\text{m}}34^{\text{s}}.93$ east of Greenwich (Gould 1853). Universal Time has then been converted to Terrestrial Time (TT) by adding a correction ΔT of $-5^{\text{s}}.20$ from *Astronomical Almanac's* online tabular data,¹⁸ based on the work by Stephenson & Morrison (1984).

(3) The orbit was integrated from Kreutz's osculation epoch of 1882 Sept 20.5 Berlin Mean Time to a standard osculation epoch of 1882 Oct 2.0 TT = JD 2408720.5.

(4) The *probable* errors of the elements used by Kreutz have been converted to the *mean* errors by applying a multiplication factor of 1.4826.

(5) A typographical error that we detected in Kreutz's paper has been corrected. It affected the published value of eccentricity, which was inconsistent with the listed logarithm of eccentricity as well as with the ratio of the perihelion distance to semimajor axis.

The orbital elements:

$$\begin{aligned} &\text{Osculation epoch 1882 October 2.0 TT} \\ T &= 1882 \text{ Sept } 17.724040 \pm 0.000047 \text{ TT} \\ \omega &= 69^{\circ}.58477 \pm 0^{\circ}.00225 \\ \Omega &= 347^{\circ}.65640 \pm 0^{\circ}.00279 \\ i &= 142^{\circ}.01104 \pm 0^{\circ}.00068 \\ q &= 0.00775020 \pm 0.00000091 \text{ AU} \\ e &= 0.99990790 \pm 0.00000021 \\ 1/a &= 0.01188356 \pm 0.00002894 \text{ AU}^{-1} \\ P &= 771.93 \pm 2.82 \text{ yr} \end{aligned}$$

The elements are based on 18 normal places in right ascension and declination (between 1882 Sept 8 and 1883 Mar 3), on an observation of the comet's ingress on the Sun's disk on 1882 Sept 17, and on 13 normal places in the coordinate perpendicular to the nuclear line (between 1882 Oct 1 and 1883 May 26). The 32 normal places, of which only five were preperihelion ones, were made up of a total of slightly more than 600 individual astrometric observations, extending over 260 days, from 1882 Sept 8 through 1883 May 26. The mean residual for a normal place of unit weight was $\pm 1''.51$.

It is interesting that in his first paper Kreutz (1888) considered the No. 2 fragment to have been a "center-of-gravity" of the disintegrated nucleus, because he was able to successfully link the preperihelion observations of the single nucleus with the post-perihelion observations of this fragment. At the time he anticipated that no other fragment would provide a similarly satisfactory linkage, but after convincing himself, in his second paper (Kreutz 1891), that the fragments Nos. 3 and 4 did as well, he changed his mind and concluded that the center of gravity could have been located anywhere along the nuclear train between the fragments Nos. 2 and 4. This

led him to maintain that the comet's pre-fragmentation orbital period was between 770 and about 1000 years. Yet, it appears that he attached more weight to the lower limit, which follows from the fact that in his third and final paper (Kreutz 1901) he returned to the problem of the comet of 1106. Even though he did mention suggestions by some astronomers that this comet might have been an earlier appearance of the 1843 sungrazer, Kreutz's preference in favor of the identity between the 1882 and 1106 comets based on the latter's daytime observations gets across as substantial.

REFERENCES

- A'Hearn, M. F., Belton, M. J. S., Delamere, W. A., et al. 2011, *Science*, 332, 1396
 Andrews, A. D. 1965, *IAU Circ.*, 1937
 Bailey, M. E., Chambers, J. E., & Hahn, G. 1992, *A&A*, 257, 315
 Benecchi, S. D., Porter, S. B., Buie, M. W., et al. 2019, *Icarus*, 334, 11
 Bessel, F. W. 1836, *Astron. Nachr.*, 13, 345
 England, K. J. 2002, *J. Brit. Astron. Assoc.*, 112, 13
 Everhart, E., & Raghavan, N. 1970, *AJ*, 75, 258
 Fernández, J. A., Lemos, P., & Gallardo, T. 2021, *Mon. Not. Roy. Astron. Soc.*, 508, 789
 Festou, M., Rickman, H., & Kamél, L. 1990, in *Asteroids, Comets, Meteors III*, ed. C.-I. Lagerkvist, H. Rickman, B. A. Lindblad, & M. Lindgren (Uppsala: Uppsala University), 313
 Gingerich, O. 1965, *IAU Circ.*, 1943 and 1946
 Goldreich, P., Lithwick, Y., & Sari, R. 2002, *Nature*, 420, 643
 Gould, B. A. 1853, *AJ*, 3, 17
 Grundy, W. M., Bird, M. K., Britt, D. T., et al. 2020, *Science*, 367, 3705
 Hall, M. 1883, *Observatory*, 6, 233
 Harmon, J. K., Nolan, M. C., Giorgini, J. D., et al. 2010, *Icarus*, 207, 499
 Hasegawa, I. 1980, *Vistas Astron.*, 24, 59
 Hasegawa, I., & Nakano, S. 2001, *Publ. Astron. Soc. Japan*, 53, 931
 Hirayama, T., & Moriyama, F. 1965, *Publ. Astron. Soc. Japan*, 17, 433
 Ho, P.-Y. 1962, *Vistas Astron.*, 5, 127
 Hubbard, J. S. 1852, *AJ*, 2, 153
 Hufnagel, L. 1919, *Astron. Nachr.*, 209, 17
 Jorda, L., Gaskell, R., Capanna, C., et al. 2016, *Icarus*, 277, 257
 Jutzi, M., & Asphaug, E. 2015, *Science*, 348, 1355
 Kanda, S. 1935, *Nihon Temmon Shiryo (Astronomical Materials in Japanese History)*, Tokyo. (In Japanese)
 Kreutz, H. 1888, *Publ. Sternw. Kiel*, 3
 Kreutz, H. 1891, *Publ. Sternw. Kiel*, 6
 Kreutz, H. 1901, *Astron. Abhandl.*, 1, 1
 Kronk, G. W. 1999, *Cometography: Volume 1 (Ancient–1799)*. Cambridge, UK: Cambridge University Press, 580 pp
 Levison, H. F., Dones, L., & Duncan, M. J. 2001, *AJ*, 121, 2253
 Lourens, J. v. B. 1966, *Mon. Not. Astron. Soc. South Africa*, 25, 52
 Marsden, B. G. 1965, *IAU Circ.*, 1947
 Marsden, B. G. 1967, *AJ*, 72, 1170
 Marsden, B. G. 1989, *AJ*, 98, 2306
 Marsden, B. G., & Williams, G. V. 2008, *Catalogue of Cometary Orbits 2008*, 17th ed. Cambridge, MA: Minor Planet Center/Central Bureau for Astronomical Telegrams, 195pp
 Marsden, B. G., Sekanina, Z., & Everhart, E. 1978, *AJ*, 83, 64
 Marsden, B. G., Sekanina, Z., & Yeomans, D. K. 1973, *AJ*, 78, 211
 McKinnon, W. B., Richardson, D. C., Marohnic, J. C., et al. 2020, *Science*, 367, 6620
 Nicolai, B. 1843, *Astron. Nachr.*, 20, 349
 Pereyra, Z. M. 1971, *AJ*, 76, 495
 Pingré, A. G. 1783, *Cométographie ou Traité historique et théorique des comètes*. Tome Premier. Paris: Imprimerie Royale
 Pohn, H. 1965, *IAU Circ.*, 1937
 Porter, J. G. 1967, *Quart. J. Roy. Astron. Soc.*, 8, 274
 Rickman, H. 1986, in *The Comet Nucleus Sample Return Mission*, ESA SP-249, ed. O. Melita (Noordwijk, Netherlands: ESTEC), 195
 Rickman, H., Froeschlé, C., Kamél, L., & Festou, M. C. 1992, *AJ*, 102, 1446
 Rickman, H., Kamél, L., Festou, M. C., & Froeschlé, C. 1987, in *Diversity and Similarity of Comets*, ESA SP-278, ed. E. J. Rolfe & B. Batrrick (Noordwijk, Netherlands: ESTEC), 471

¹⁸ See a website: <https://webservice.science.uu.nl/~gent0113/deltat/deltat.htm>.

- Rickman, H., Marchi, S., A'Hearn, M. F., et al. 2015, *A&A*, 583, A44
- Roemer, E. 1963, *Publ. Astron. Soc. Pacific*, 75, 535
- Roemer, E. 1965, *AJ*, 70, 397
- Roemer, E., & Lloyd, R. E. 1966, *AJ*, 71, 443
- Schaefer, B. E. 1993, *Vistas Astron.*, 36, 311
- Schaefer, B. E. 1998, *Sky Tel.*, 95, 57; code version by L. Bogan at <https://www.bogan.ca/astro/optics/vislimit.html>
- Sekanina, Z. 1982, in *Comets*, ed. L. L. Wilkening (Tucson: University of Arizona Press), 251
- Sekanina, Z. 1988, *AJ*, 86, 1455
- Sekanina, Z. 1992, in *Observations and Physical Properties of Small Solar System Bodies*, *Proc. Liège Internat. Astrophys. Coll. No. 30*, ed. A. Brahic, J.-C. Gérard, & A. Surdej (Liège: Université de Liège, Institut d'Astrophysique), 133
- Sekanina, Z. 1993, *AJ*, 105, 702
- Sekanina, Z. 2002, *ApJ*, 566, 577
- Sekanina, Z. 2021, eprint arXiv:2109.01297 (Paper 1)
- Sekanina, Z. 2022, eprint arXiv:2202.01164 (Paper 2)
- Sekanina, Z., & Chodas, P. W. 2002, *ApJ*, 581, 760
- Sekanina, Z., & Chodas, P. W. 2004, *ApJ*, 607, 620
- Sekanina, Z., & Chodas, P. W. 2007, *ApJ*, 663, 657
- Sekanina, Z., & Chodas, P. W. 2008, *ApJ*, 687, 1415
- Sekanina, Z., & Chodas, P. W. 2012, *ApJ*, 757, 127 (33 pp)
- Stephenson, F. R., & Morrison, L. V. 1984, in *Rotation in the Solar System*, ed. R. Hide (London: Royal Society), 165
- Stern, S. A., Weaver, H. A., Spencer, J. R., et al. 2019, *Science*, 364, 9771
- Strom, R. 2002, *A&A*, 387, L17
- Suresh, S. 2004, *Fatigue of Materials*. (2nd ed.) Cambridge, UK: Cambridge University Press, 703pp
- Tammann, G. A. 1966, *IAU Circ.*, 1952
- Yeomans, D. K., & Chodas, P. W. 1989, *AJ*, 98, 1083